

2017 Autumn School on Correlated Electrons
The Physics of Strongly Correlated Insulators, Metals, and Superconductors
Forschungszentrum Jülich 25-29 September 2017

Hund's metals, explained

Luca de' Medici



Hund's metals

LETTERS

PUBLISHED ONLINE: 18 SEPTEMBER 2011 | DOI: 10.1038/NMAT3120

nature
materials

Kinetic frustration and the nature of the magnetic and paramagnetic states in iron pnictides and iron chalcogenides

Z. P. Yin^{1,2*}, K. Haule¹ and G. Kotliar¹

The iron pnictide and chalcogenide compounds are a subject of intensive investigations owing to their surprisingly high temperature superconductivity¹. They all share the same basic building blocks, but there is significant variation in their physical properties, such as magnetic ordered moments, effective masses, superconducting gaps and transition temperature (T_c). Many theoretical techniques have been applied to individual compounds but no consistent description of the microscopic origin of these variations is available². Here we carry out a comparative theoretical study of a large number of iron-based compounds in both their magnetic and paramagnetic states. Taking into account correlation effects and realistic band structures, we describe well the trends in all of the physical properties such as the ordered moments, effective masses and Fermi surfaces across all families of iron compounds, and find them to be in good agreement with experiments. We trace variation in physical properties to variations in the key structural parameters, rather than changes in the screening of the Coulomb interactions. Our results also provide a natural explanation of the strongly Fermi-surface-dependent superconducting gaps observed in experiments³.

The iron pnictides/chalcogenides are Hund's metals. In these systems the Coulomb interaction among the electrons is not strong enough to fully localize them, but it significantly slows them down, such that low-energy emerging quasiparticles have a substantially enhanced mass⁴. This enhanced mass emerges not because of the Hubbard interaction U , but because of the Hund's rule interactions that tend to align electrons with the same spin but different orbital quantum numbers when they find themselves on the same iron atom⁴.

Although critical long-wavelength fluctuations certainly play a role near the phase-transition lines, we will show that the local fluctuations on the iron atom can account for the correct trend of magnetic moments and correlation strength in iron pnictide/chalcogenide layered compounds.

Using the combination of DFT and dynamical mean field theory (DFT + DMFT) (see Supplementary Information for details), we studied two different real-space orderings, the SDW ordering, characterized by wave vector $(\pi, 0, \pi)$ (this vector is written in coordinates with one iron atom per unit cell), which is experimentally found in iron arsenide compounds, and $(\pi/2, \pi/2, \pi)$ ordering, denoted by the double-stripe SDW (DSDW). The latter was found experimentally in FeTe. Figure 1a shows our theoretical results for the ordered moment in both phases together with experimentally determined values^{6–13} from across all known families of iron-based superconducting compounds. There is an overall good agreement between theory and experiment; in particular, LaFePO is predicted to be non-magnetic, most 1111 and 122 compounds have an ordered moment below $1.0 \mu_B$ (ref. 14) and FeTe orders with a DSDW moment of $2.1 \mu_B$.

We now explain the variation of the ordered moment in terms of real-space and momentum-space concepts. The size of the fluctuating local moment, which can be extracted from neutron scattering experiments, gives an upper bound to the size of the ordered magnetic moment and is also plotted in Fig. 1a. It was computed from the atomic histogram in Fig. 2c, which shows the percentage of time the iron 3d electrons spend in various atomic configurations when the system is still in its paramagnetic state. Only high-spin states, which carry a large weight as a result of the Hund's rule coupling in iron, are shown (see also Supplementary

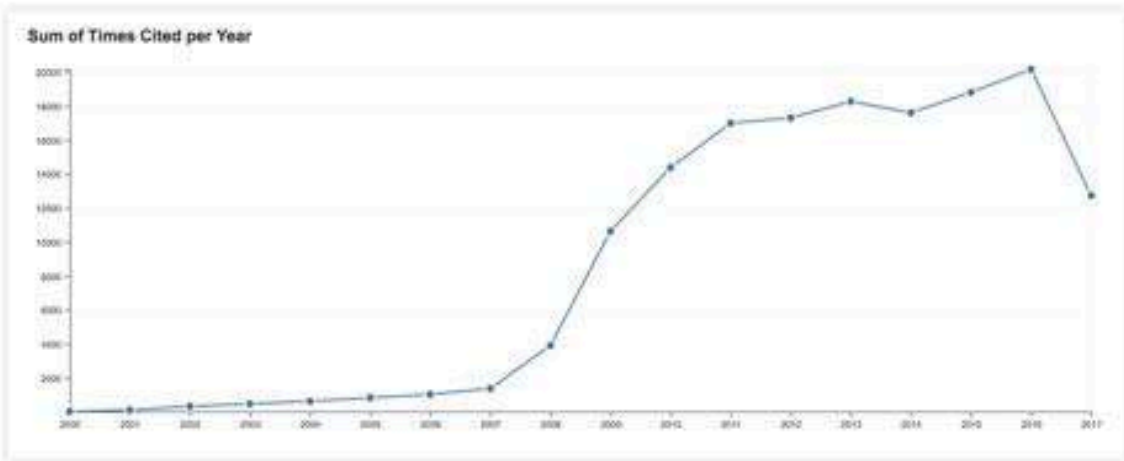
Hund's metals

You searched for: TOPIC: (iron) AND TOPIC: (superconduct*) ...More

This report reflects citations to source items indexed within Web of Science Core Collection. Perform a Cited Reference Search to include citations to items not indexed within Web of Science Core Collection.

Export Data: Save to Text ...

Total Publications 6.263 	h-index 152 Average citations per item 24,84	Sum of Times Cited 155.587 Without self citations 78.933	Citing articles 41.325 Without self citations 36.319
--	---	---	---



Sort by: Times Cited – highest to lo...

Page 1 of 627

Use the checkboxes to remove individual items from this Citation Report

or restrict to items published between 2... and 2... Go

	2014	2015	2016	2017	2018	Total	Average Citations per Year
	17609	18806	20160	12733	0	155587	8643.72
1. Iron-based layered superconductor La_{0.95-x}FxFeAs (x=0.05-0.12) with T_c=26 K	466	447	354	222	0	5302	530.20

By: Kamihara, Yoichi; Watanabe, Takumi; Hirano, Masahiro; et al.
 JOURNAL OF THE AMERICAN CHEMICAL SOCIETY Volume: 130 Issue: 11 Pages: 3296-
 Published: MAR 19 2008

Hund's metals

You searched for: TOPIC: (iron) AND TOPIC: (superconduct*) ...More

This report reflects citations to source items indexed within Web of Science Core Collection. Perform a Cross-Check to identify items indexed within Web of Science Core Collection.

nature nanotechnology

Home | Current issue | Comment | Research | Archive | Authors & referees | About the journal

home > archive > issue > news and views > full text

NATURE NANOTECHNOLOGY | NEWS AND VIEWS

Magnetic atoms: The makings of a Hund's metal

Cyrus F. Hirjibehedin

Nature Nanotechnology 10, 914–915 (2015) | doi:10.1038/nnano.2015.225

Published online 04 November 2015

Page 1 of 627

Use the checkboxes to remove individual items from this Citation Report

or restrict to items published between 2... and 2... Go

	2014	2015	2016	2017	2018	Total	Average Citations per Year
	17609	18806	20160	12733	0	155587	8643.72
1. Iron-based layered superconductor La[O_{1-x}F_x]FeAs (x=0.05-0.12) with T_c=26 K	466	447	354	222	0	5302	530.20

By: Kamihara, Yoichi; Watanabe, Takumi; Hirano, Masahiro; et al.
JOURNAL OF THE AMERICAN CHEMICAL SOCIETY Volume: 130 Issue: 11 Pages: 3296-
Published: MAR 19 2008

Hund's metals

You searched for: TOPIC: (iron) AND TOPIC: (superconduct*) ...More

This report reflects citations to source items indexed within Web of Science Core Collection. Perform a Citations Report on items indexed within Web of Science Core Collection.

week ending
9 DECEMBER 2016

nature
nanotechnology

Home | Current issue | Comment | Research | Archive | Authors & Editors

home > archive > issue > news and views > full text articles

NATURE NANOTECHNOLOGY

PHYSICAL REVIEW LETTERS

PRL 117, 247001 (2016)

Orbital-Dependent Band Narrowing Revealed in an Extremely Correlated Hund's Metal

Takeshi Kondo,¹ M. Ochi,^{2,3} M. Nakayama,¹ H. Taniguchi,^{4,5} S. Akebi,¹ K. Kuroda,¹ M. Arita,⁶
S. Sakai,³ H. Namatame,⁶ M. Taniguchi,^{6,7} Y. Maeno,⁵ R. Arita,³ and S. Shin¹

November 2015

doi:10.1038/nnano.2015.225

Page 1 of 627

	2014	2015	2016	2017	2018	Total	Average Citations per Year
17609	18806	20160	12733	0	155587	8643.72	
1. Iron-based layered superconductor La[O _{1-x} Fx]FeAs (x=0.05-0.12) with T _c =26 K	466	447	354	222	0	5302	530.20

Use the checkboxes to remove individual items from this Citation Report

or restrict to items published between 2... and 2... Go

By: Kamihara, Yoichi; Watanabe, Takumi; Hirano, Masahiro; et al
JOURNAL OF THE AMERICAN CHEMICAL SOCIETY Volume: 130 Issue: 11 Pages: 3296-
Published: MAR 19 2008

Hund's metals

You searched for: TOPIC: (iron) AND TOPIC: (superconduct*) ...More

This report reflects citations to source items indexed within Web of Science Core Collection. Perform a search on the source items indexed within Web of Science Core Collection.

nature nanotechnology

Home | Current | home » arch

NATURE NANOTECHNOLOGY

PRL 117, 247001 (2016)

Orbital-Dependent Kondo Effect in LaFePO_4

Takeshi Kondo,¹ Naoki S. Sakai,^{1,2} ...

EXTRA! EXTRA!
READ ALL ABOUT IT!
HUND'S METALS!

week ending 9 DECEMBER 2016

Hund's Metal

6

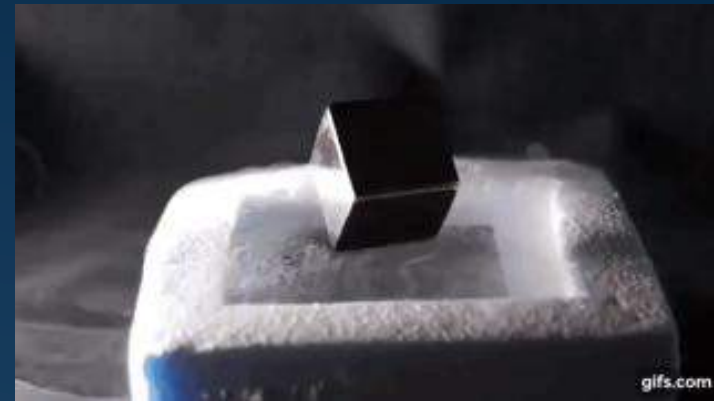
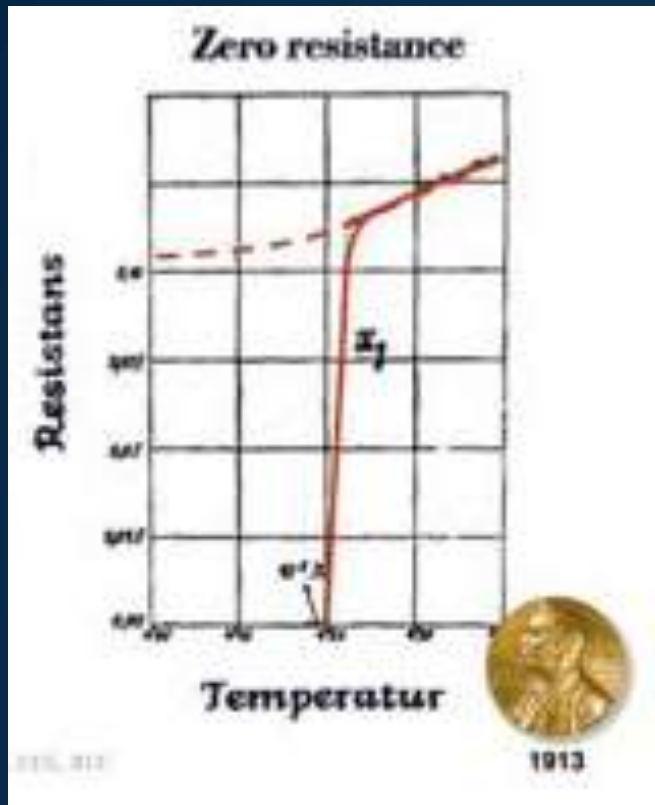
Page 1 of 627

Year	2014	2015	2016	2017	2018	Total	Average Citations per Year
	17609	18806	20160	12733	0	155587	8643.72
1. Iron-based layered superconductor $\text{La}[\text{O}1-x]$	466	447	354	222	0	5302	530.20

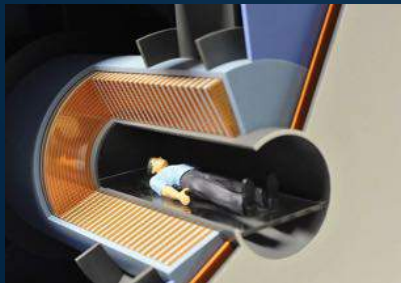
Use the checkboxes to remove items or restrict to items published between ...

1. Iron-based layered superconductor $\text{La}[\text{O}1-x]$...
By: Kamihara, Yoichi; Watanabe, Takumi; Hirano, ...
JOURNAL OF THE AMERICAN CHEMICAL SOCIETY Volume: 130 Issue: 11 Pages: 3296-
Published: MAR 19 2008

Superconducting materials



Magnetic Resonance Imaging

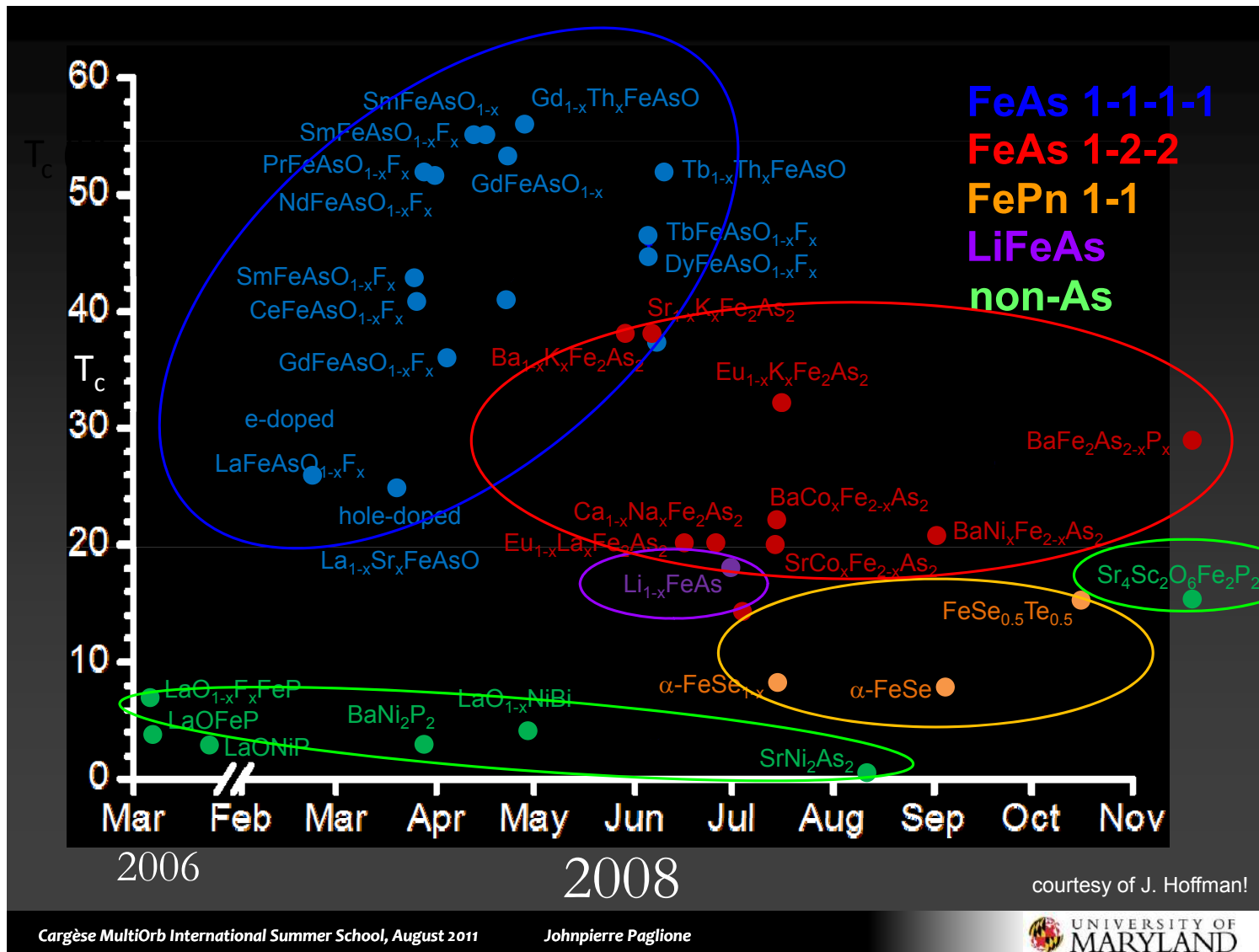


Energy transportation



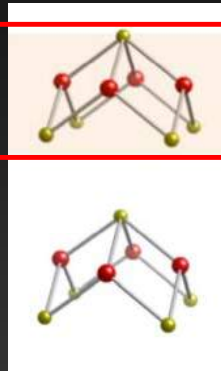
MAGLEV technology

Iron-based superconductors

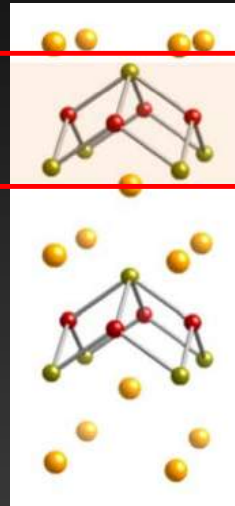


Iron-based superconductors

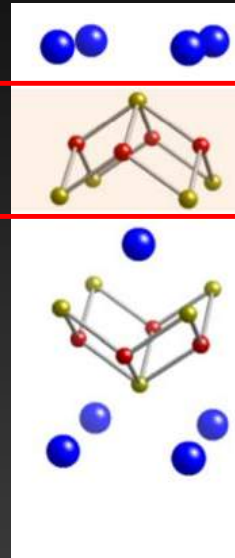
Crystal Structures



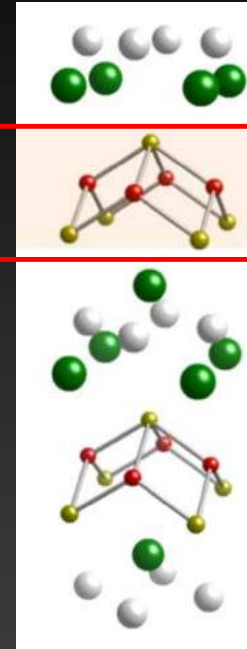
FeSe



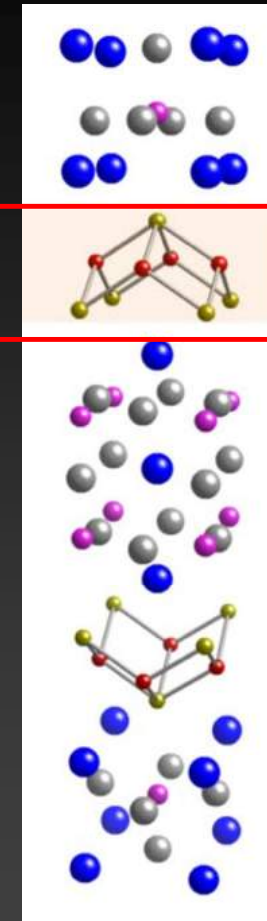
LiFeAs



BaFe₂As₂



LaOFeAs



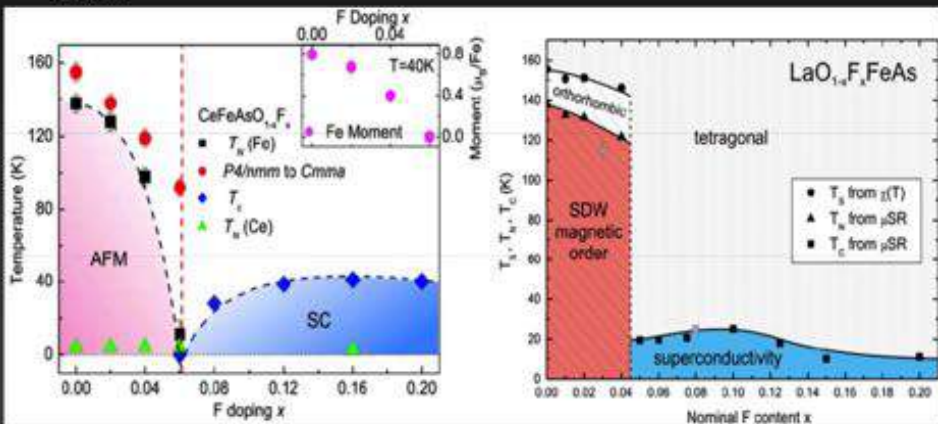
Sr₃Sc₂O₅Fe₂As₂

Paglione/Greene review (2010)

- relevant block: Fe-ligand (As, Se, Te) buckled plane
- tetragonal – orthorhombic symmetry

el-doped 1111

$RO_{1-x}F_xFeAs$



J. Zhao et al. (2008)

H. Luetkens et al. (2008)

hole-doped 122

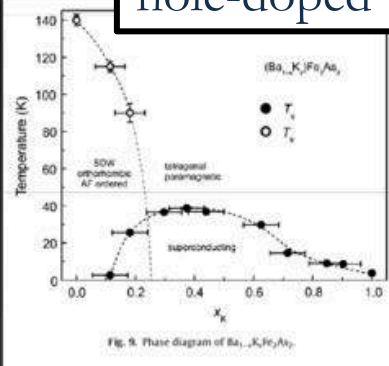


Fig. 9. Phase diagram of $Ba_{1-x}K_xFe_2As_2$

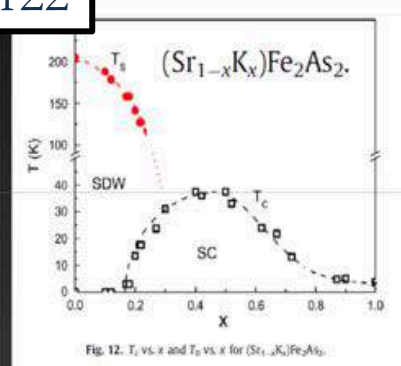
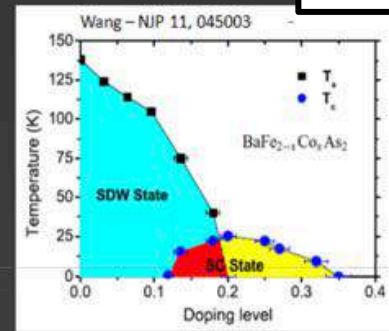
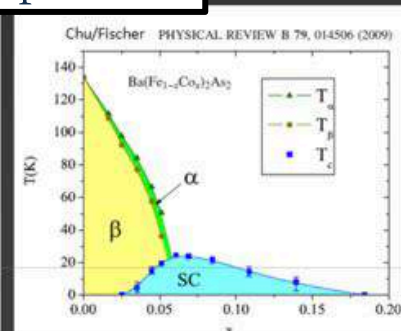


Fig. 12. T_N vs. x and T_c vs. x for $(Sr_{1-x}K_x)Fe_2As_2$.

el-doped 122

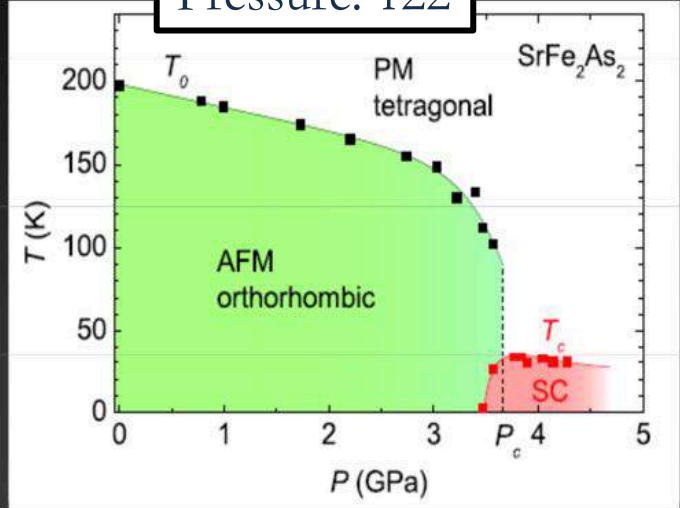


Wang - NJP 11, 045003



Chu/Fischer - PHYSICAL REVIEW B 79, 014506 (2009)

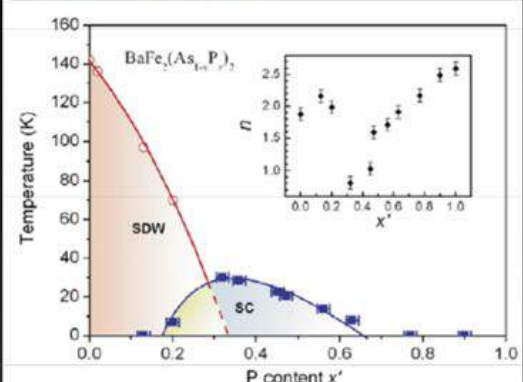
Pressure: 122



H. Kotegawa et al. (2008)

Shuai Jiang

J. Phys.: Condens. Matter 21 (2009) 382203



Isovalent doping:
122

el-doped 1111

hole-doped 122

$RO_{1-x}F_xFeAs$

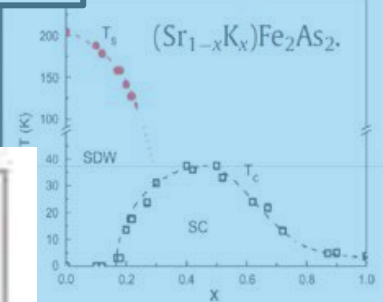
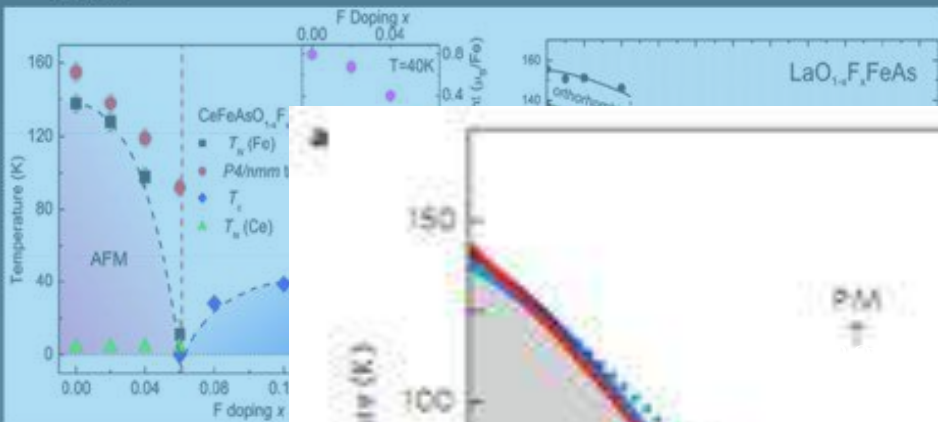
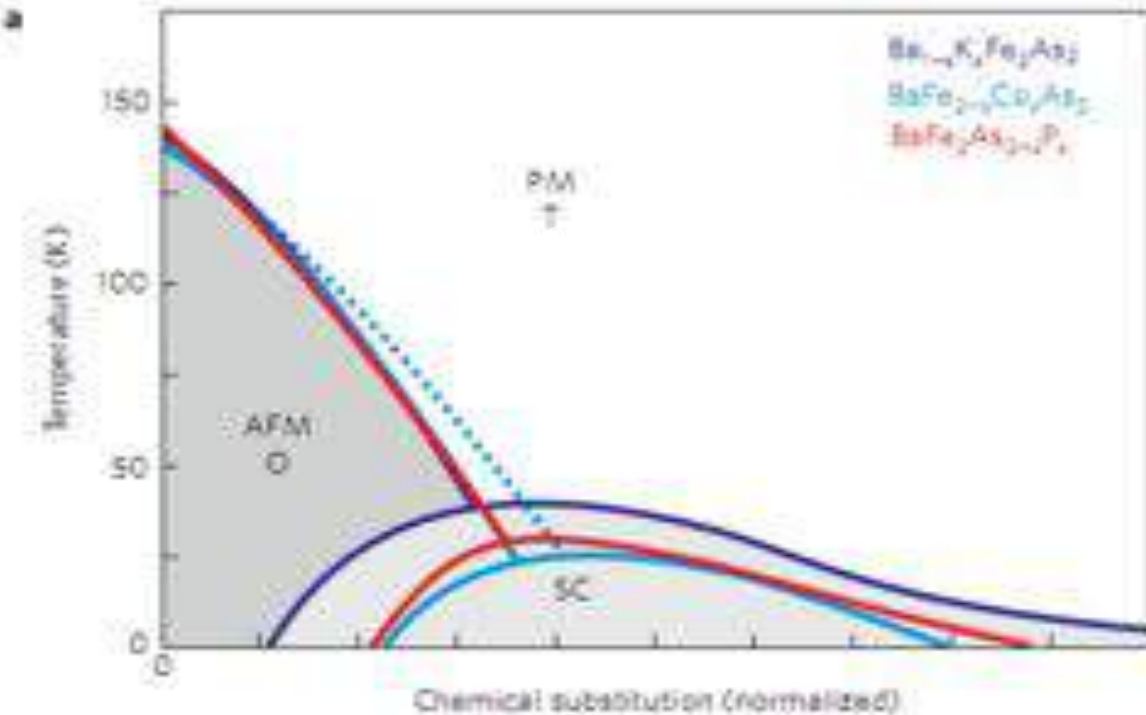
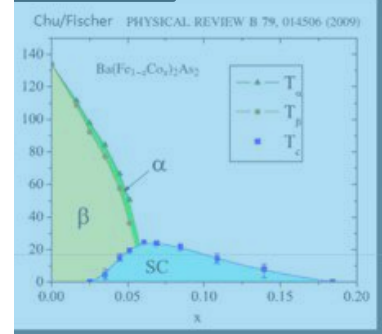


Fig. 12. T_N vs. x and T_c vs. x for $(Sr_{1-x}K_x)Fe_2As_2$.

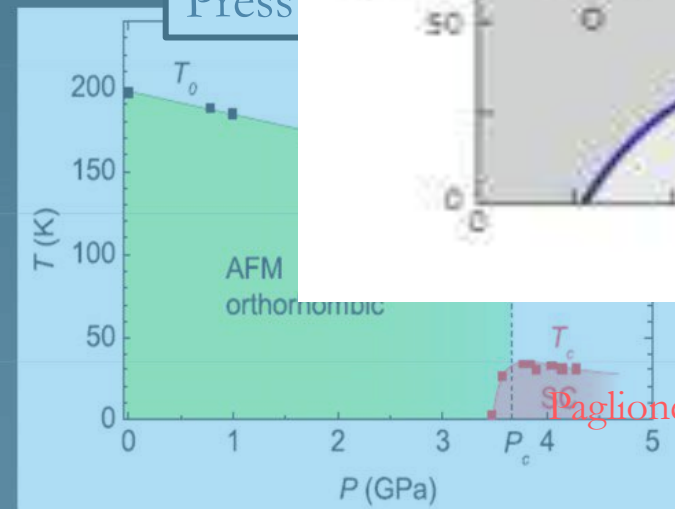


ed 122



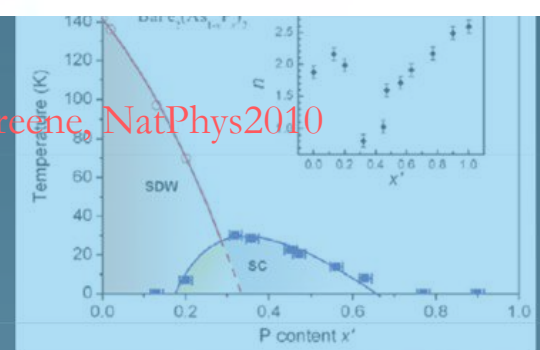
Chu/Fischer PHYSICAL REVIEW B 79, 014506 (2009)

Press

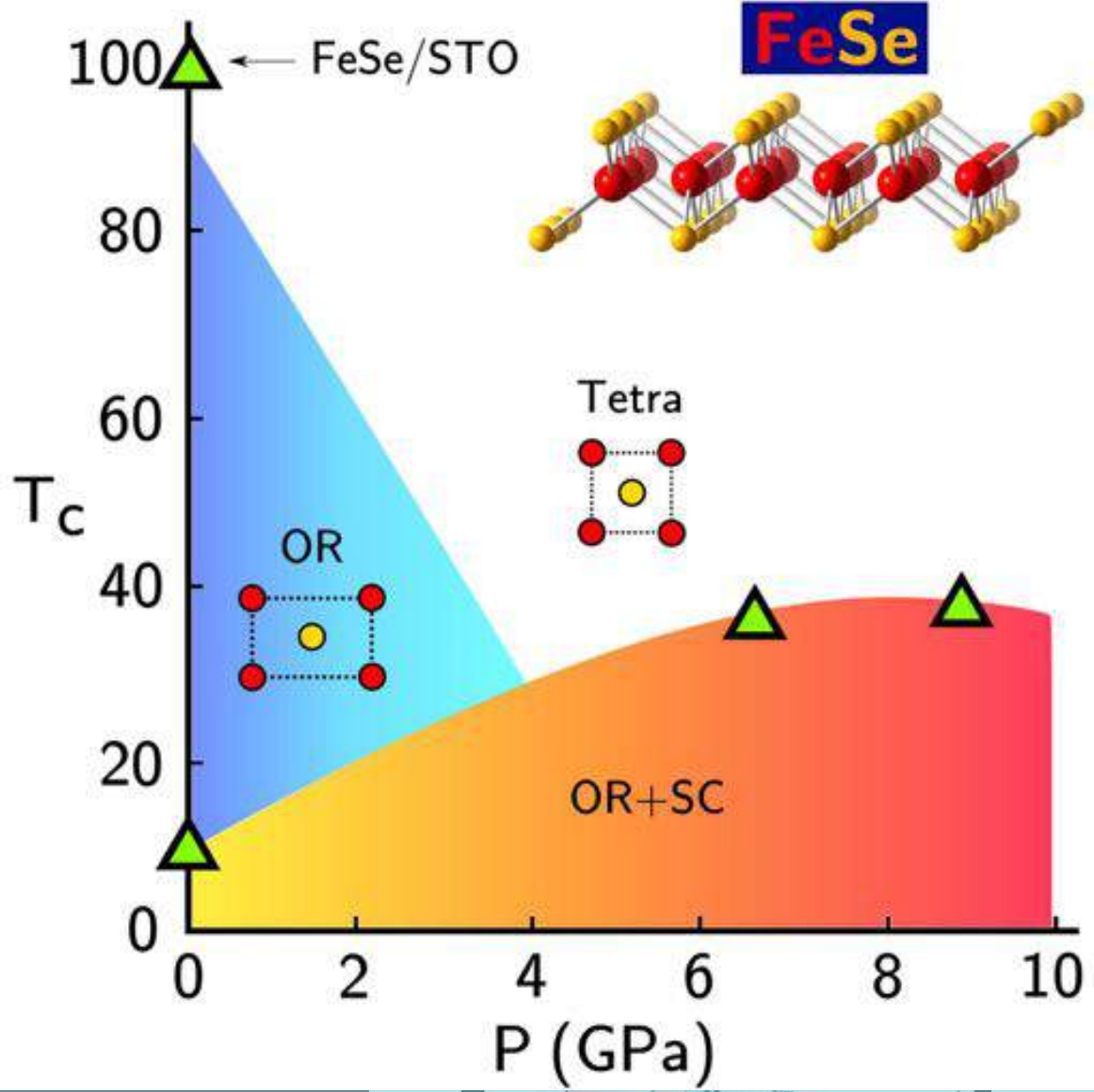


H. Kotegawa et al. (2008)

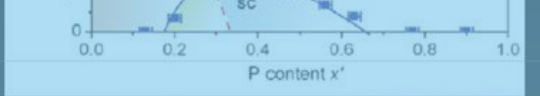
Paglione and Greene, NatPhys2010



Isovalent doping:
122

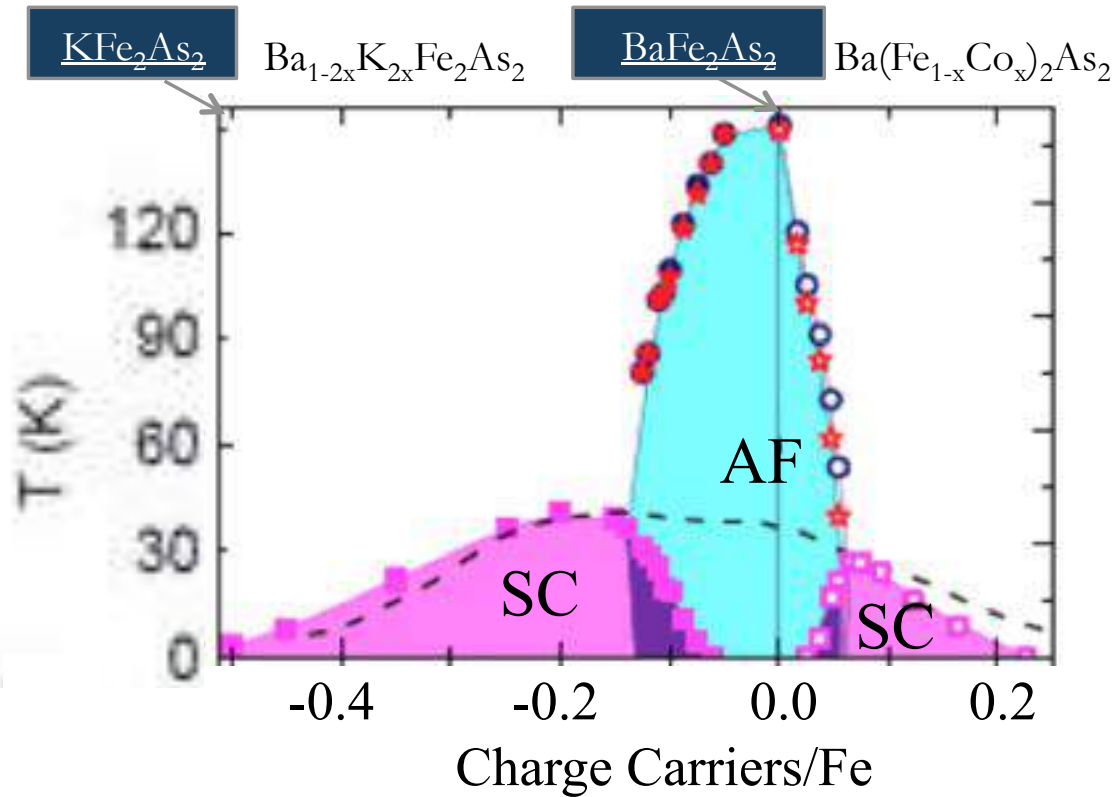


H. Kotegawa *et al.* (2008)

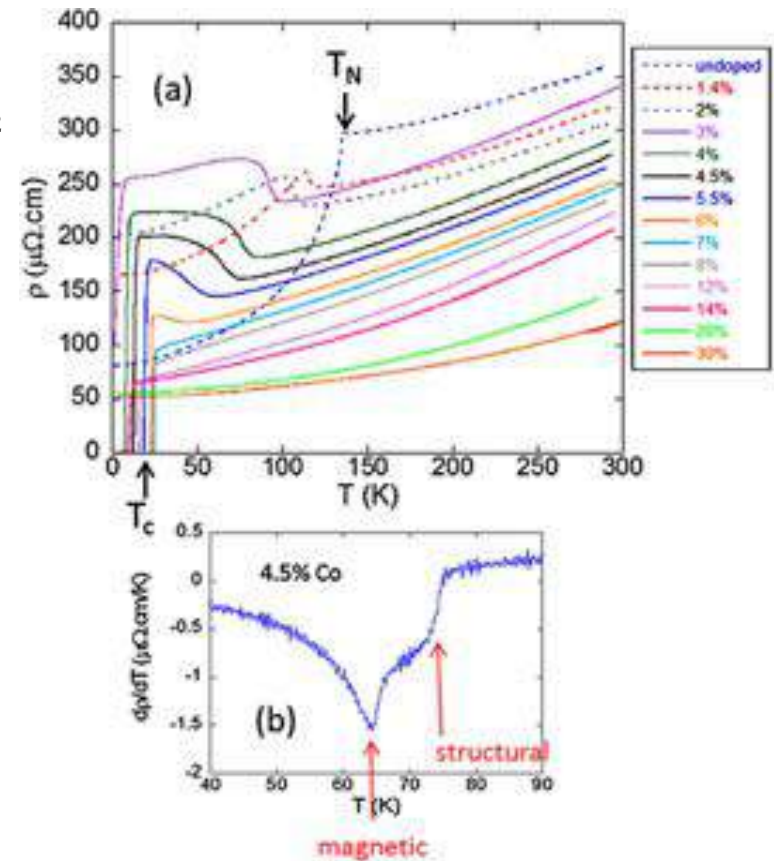


Multi-orbital fermi-liquid metals

The “122” family



Auci et al. PRB 85 (2012)



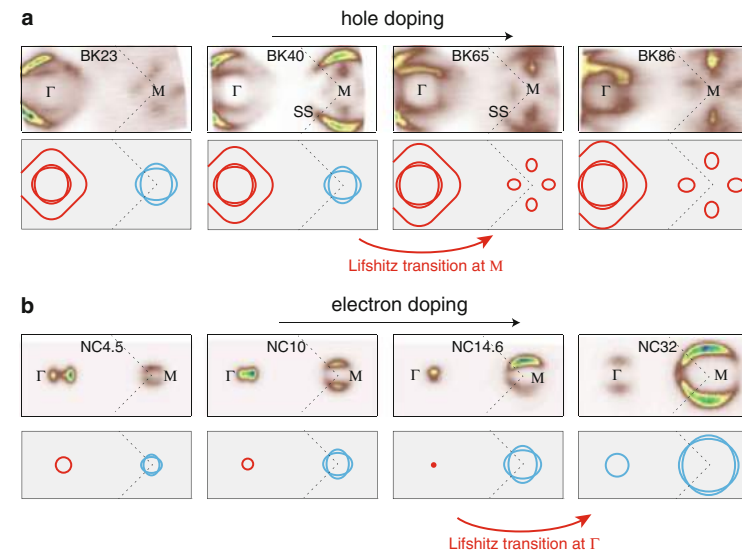
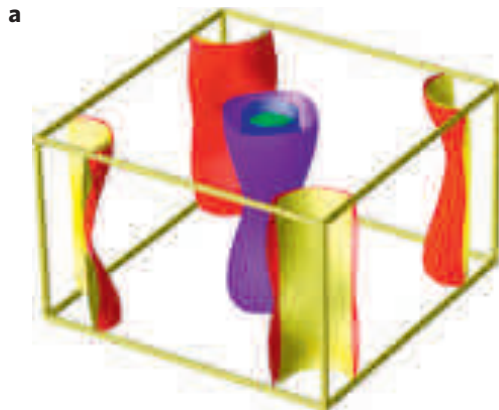
F. Rullier-Albenque, Comptes Rendus Physique 17 (2016) 164-187

Theoretical approaches: itinerant electrons

- multi-orbital: 5 bands (Fe 3d) at the Fermi level ($W \sim 4\text{eV}$)
 $n=6$ conduction electrons
- Partially lifted degeneracy (crystal-field splitting $\sim 0.4\text{eV}$)

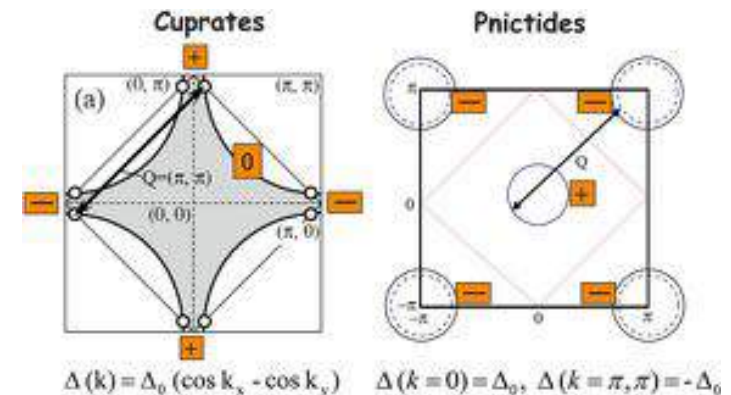
Zhang et al.,
Springer Book 2015

Mazin and Schmalian, Physica C 2009



Itinerant electrons:

- DFT gives correct FS topology (semi-compensated metal)
- Nesting of FS pockets provides SDW and spin-fluctuations induce SC pairing (S^\pm -wave)

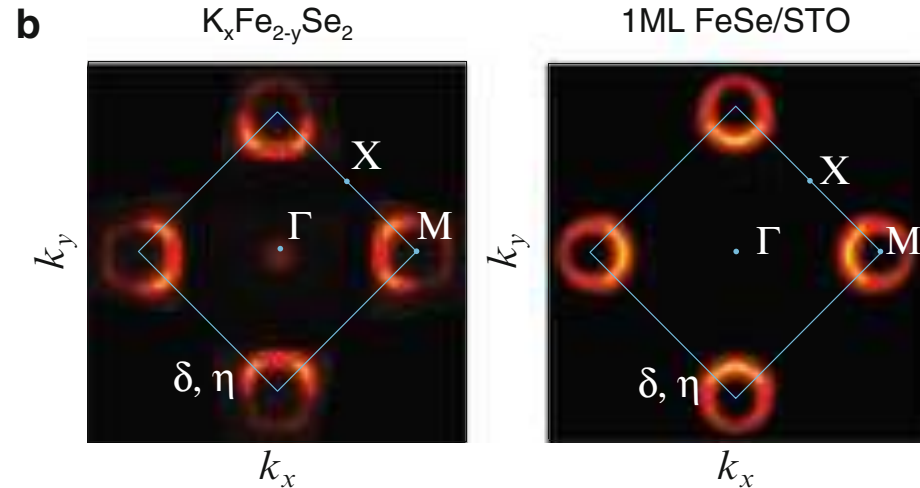
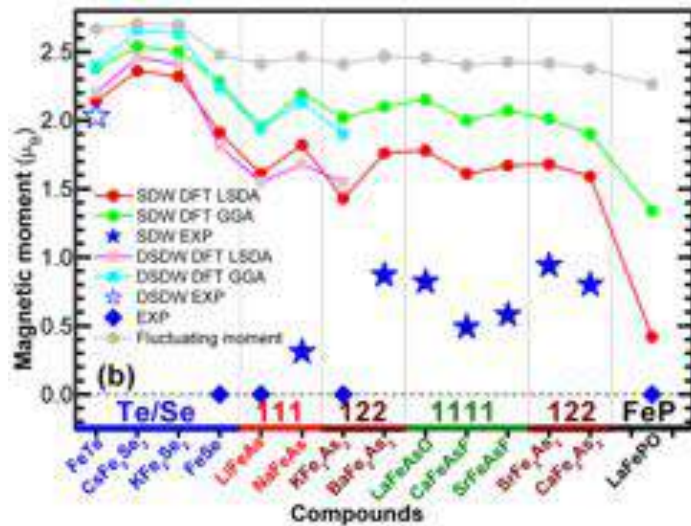


A. Chubukov, Springer Book 2015

Problems of the itinerant model

Yin et al. Nat. Mat. 2011

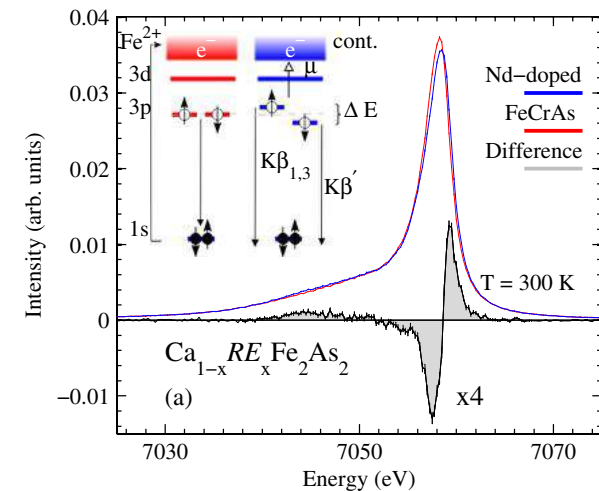
Zhang et al. Nat Mat 10 (2011) Tan et al. Nat Mat 12 (2014)



Problems

- DFT bands 2-3 times too dispersive
- LSDA unusually overestimates the ordered magnetic moment
- FeSe ($T_c=8K$) and LiFeAs ($T_c=18K$) do not have magnetic order
- $K_xFe_{2-y}Se_2$ ($T_c\sim 40K$) and FeSe monolayer ($T_c\sim 100K??$) only have electron pockets. KFe_2As_2 ($T_c=4K$) only hole pockets.
- Direct evidence of local moments in the PM phase (XES)

Electronic Correlations?



XES: Gretarsson et al. PRB 2011

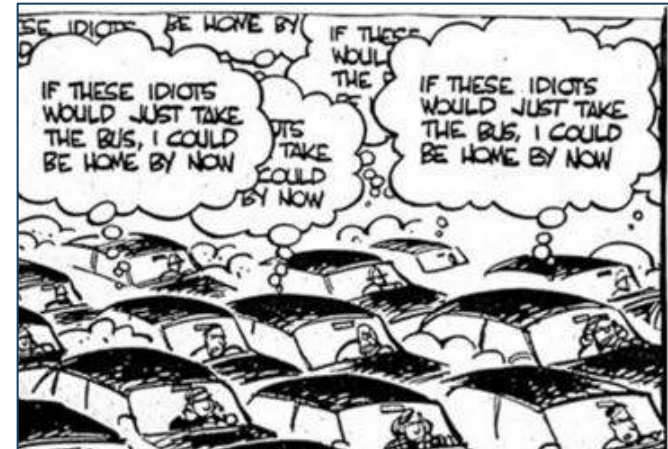
Correlated Materials

Band theory

Fermi-liquid, enhanced masses, instabilities, local magnetism,...

Mott insulator

increasing electronic correlations



Unconventional phenomena:

- High-T_c superconductivity
- large thermoelectric responses
- colossal magnetoresistance, ...

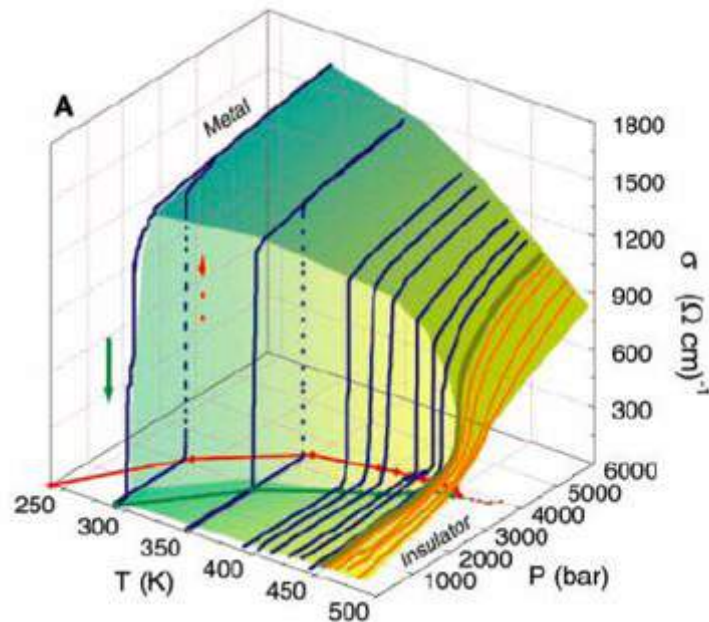
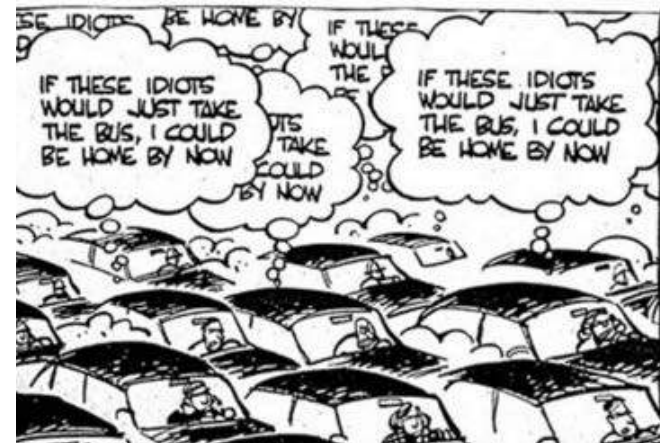
Materials typically from 3d and 4f open shells: Cuprates, Fe-based superconductors, Manganites, heavy-fermions,...

1	2	3	4	5	6	7	8	9	10	11	12	13	14	15	16	17	18														
1 hydrogen H 1.00794(7)																	2 helium He 4.002602(2)														
3 lithium Li 6.941(2)	4 beryllium Be 9.012182(3)											5 boron B 10.811(7)	6 carbon C 12.0107(8)	7 nitrogen N 14.00642(7)	8 oxygen O 15.999(4)	9 fluorine F 18.9984032(3)	10 neon Ne 20.1797(6)														
11 sodium Na 22.989770(2)	12 magnesium Mg 24.305(6)											13 aluminum Al 26.981538(6)	14 silicon Si 28.0855(3)	15 phosphorus P 30.9737612(2)	16 sulfur S 32.06(6)	17 chlorine Cl 35.452(9)	18 argon Ar 39.948(1)														
19 potassium K 39.0983(1)	20 calcium Ca 40.078(4)	21 scandium Sc 44.955910(8)	22 titanium Ti 47.867(1)	23 vanadium V 50.9415(1)	24 chromium Cr 51.9961(6)	25 manganese Mn 54.938049(9)	26 iron Fe 55.845(2)	27 cobalt Co 58.933200(9)	28 nickel Ni 58.6934(2)	29 copper Cu 63.546(3)	30 zinc Zn 65.39(2)	31 gallium Ga 72.61(2)	32 germanium Ge 72.61(2)	33 arsenic As 74.921602(2)	34 selenium Se 78.96(3)	35 bromine Br 79.904(1)	36 krypton Kr 83.80(1)														
37 rubidium Rb 85.4678(3)	38 strontium Sr 87.62(1)	39 yttrium Y 88.90585(2)	40 zirconium Zr 91.224(2)	41 niobium Nb 92.90638(2)	42 molybdenum Mo 95.94(1)	43 technetium Tc 98.9063(8)	44 ruthenium Ru 101.07(2)	45 rhodium Rh 102.90550(2)	46 palladium Pd 106.42(1)	47 silver Ag 107.8682(2)	48 cadmium Cd 112.411(8)	49 indium In 114.818(3)	50 tin Sn 118.710(7)	51 antimony Sb 121.760(1)	52 tellurium Te 127.60(3)	53 iodine I 126.90447(3)	54 xenon Xe 131.29(2)														
55 cesium Cs 132.90545(2)	56 barium Ba 137.327(7)	57-70 lanthanum La 138.905(2)	71 cerium Ce 140.116(1)	72 praseodymium Pr 140.90768(2)	73 neodymium Nd 144.242(3)	74 promethium Pm 144.9127(7)	75 samarium Sm 150.36(3)	76 europium Eu 151.964(1)	77 gadolinium Gd 157.25(3)	78 terbium Tb 158.92547(2)	79 dysprosium Dy 162.50(3)	80 holmium Ho 164.93032(2)	81 erbium Er 167.258(3)	82 thulium Tm 168.93402(2)	83 ytterbium Yb 173.04(3)	84 lutetium Lu 174.967(1)	85 hafnium Hf 178.49(2)	86 tantalum Ta 180.9479(1)	87 tungsten W 183.84(1)	88 rhenium Re 186.207(1)	89 osmium Os 190.23(3)	90 iridium Ir 192.222(3)	91 platinum Pt 195.078(2)	92 gold Au 196.96656(2)	93 mercury Hg 200.59(2)	94 thallium Tl 204.3833(2)	95 lead Pb 207.21(1)	96 bismuth Bi 208.98039(2)	97 polonium Po 209.984(1)	98 astatine At [208.9871]	99 radon Rn [222.0176]
87 francium Fr [223.0187]	88 radium Ra [226.0254]	89-102 actinides	103 lawrencium Lr [262.110]	104 rutherfordium Rf [261.1089]	105 dubnium Db [263.1144]	106 seaborgium Sg [263.1166]	107 bohrium Bh [264.12]	108 hassium Hs [265.1309]	109 meitnerium Mt [268]	110 darmstadtium Ds [269]	111 roentgenium Rg [272]	112 copernicium Cn [277]	113 nihonium Nh [284]	114 flerovium Fl [289]	115 moscovium Mc [290]	116 livermorium Lv [293]	117 tennessine Ts [294]	118 oganeson Og [294]	119 unbinilium Uub [295]	120 ununilium Uuq [296]	121 unununium Uuu [297]	122 ununbium Uub [298]	123 ununtrium Uut [299]	124 ununquadium Uuq [300]	125 ununpentium Uup [301]	126 ununhexium Uuh [302]	127 ununseptium Uus [303]	128 ununoctium Uuo [304]	129 ununennium Uue [305]	130 unbinilium Uub [306]	
57 lanthanum La 138.905(2)	58 cerium Ce 140.116(1)	59 praseodymium Pr 140.90768(2)	60 neodymium Nd 144.242(3)	61 promethium Pm 144.9127(7)	62 samarium Sm 150.36(3)	63 europium Eu 151.964(1)	64 gadolinium Gd 157.25(3)	65 terbium Tb 158.92547(2)	66 dysprosium Dy 162.50(3)	67 holmium Ho 164.93032(2)	68 erbium Er 167.258(3)	69 thulium Tm 168.93402(2)	70 ytterbium Yb 173.04(3)	71 lutetium Lu 174.967(1)	72 hafnium Hf 178.49(2)	73 tantalum Ta 180.9479(1)	74 tungsten W 183.84(1)	75 rhenium Re 186.207(1)	76 osmium Os 190.23(3)	77 iridium Ir 192.222(3)	78 platinum Pt 195.078(2)	79 gold Au 196.96656(2)	80 mercury Hg 200.59(2)	81 thallium Tl 204.3833(2)	82 lead Pb 207.21(1)	83 bismuth Bi 208.98039(2)	84 polonium Po [208.9871]	85 astatine At [208.9871]	86 radon Rn [222.0176]		
89 actinides	90 thorium Th [232.0377]	91 protactinium Pa [231.03688(2)]	92 uranium U [238.02891(3)]	93 neptunium Np [237.048173(3)]	94 plutonium Pu [244.06422(3)]	95 americium Am [243.0614(3)]	96 curium Cm [247.0703(3)]	97 berkelium Bk [247.0703(3)]	98 californium Cf [251.0788(3)]	99 einsteinium Es [252.083(3)]	100 fermium Fm [257.103(3)]	101 mendelevium Md [258.103(3)]	102 nobelium No [259.103(3)]	103 lawrencium Lr [260.103(3)]	104 rutherfordium Rf [261.103(3)]	105 dubnium Db [262.103(3)]	106 seaborgium Sg [263.103(3)]	107 bohrium Bh [264.103(3)]	108 hassium Hs [265.103(3)]	109 meitnerium Mt [266.103(3)]	110 darmstadtium Ds [267.103(3)]	111 roentgenium Rg [268.103(3)]	112 copernicium Cn [269.103(3)]	113 nihonium Nh [270.103(3)]	114 flerovium Fl [271.103(3)]	115 moscovium Mc [272.103(3)]	116 livermorium Lv [273.103(3)]	117 tennessine Ts [274.103(3)]	118 oganeson Og [275.103(3)]	119 unbinilium Uub [276.103(3)]	120 ununilium Uuq [277.103(3)]

Mott Transition

Localization of conduction electrons by correlations

Relevant for transition metal oxides,
Fullerenes, organic superconductors,...



Limelette et al. Science 302, 89 (2003)

The proximity to a Mott state strongly affects
the properties of a system:

- reduced metallicity (Fermi-liquid: quasiparticle effective mass)
- transfer of spectral weight from low to high energy (e.g. in optical response)
- tendency towards magnetism
- ...

Band Theory of electrons in a solid

$$\hat{H} = - \sum_i \frac{\hbar^2 \nabla_i^2}{2m_e} - \sum_{i\alpha} \frac{Z_\alpha e^2}{|\mathbf{R}_\alpha - \mathbf{r}_i|} + \frac{1}{2} \sum_{i \neq i'} \frac{e^2}{|\mathbf{r}_i - \mathbf{r}_{i'}|}$$

Independent electron
approximation

$$\hat{h}(\mathbf{r}_i) \equiv \frac{\hbar^2 \nabla_i^2}{2m_e} + v_{eff}(\mathbf{r}_i)$$

one-particle
Schrödinger equation

$$\hat{h}(\mathbf{r})\phi_a(\mathbf{r}) = \epsilon_a\phi_a(\mathbf{r})$$

In a translationally invariant system (crystal)

Bloch Functions $\phi_a(\mathbf{r}) \equiv \phi_{\mathbf{k}n}(\mathbf{r}) = e^{i\mathbf{k}\cdot\mathbf{r}} u_{n\mathbf{k}}(\mathbf{r})$

Many-body wave function

Band theory: factorized many-body wave function

$$\psi(\mathbf{x}_1, \mathbf{x}_2) = \phi_a(\mathbf{x}_1)\phi_b(\mathbf{x}_2) \quad E = \epsilon_a + \epsilon_b$$

Antisymmetrization

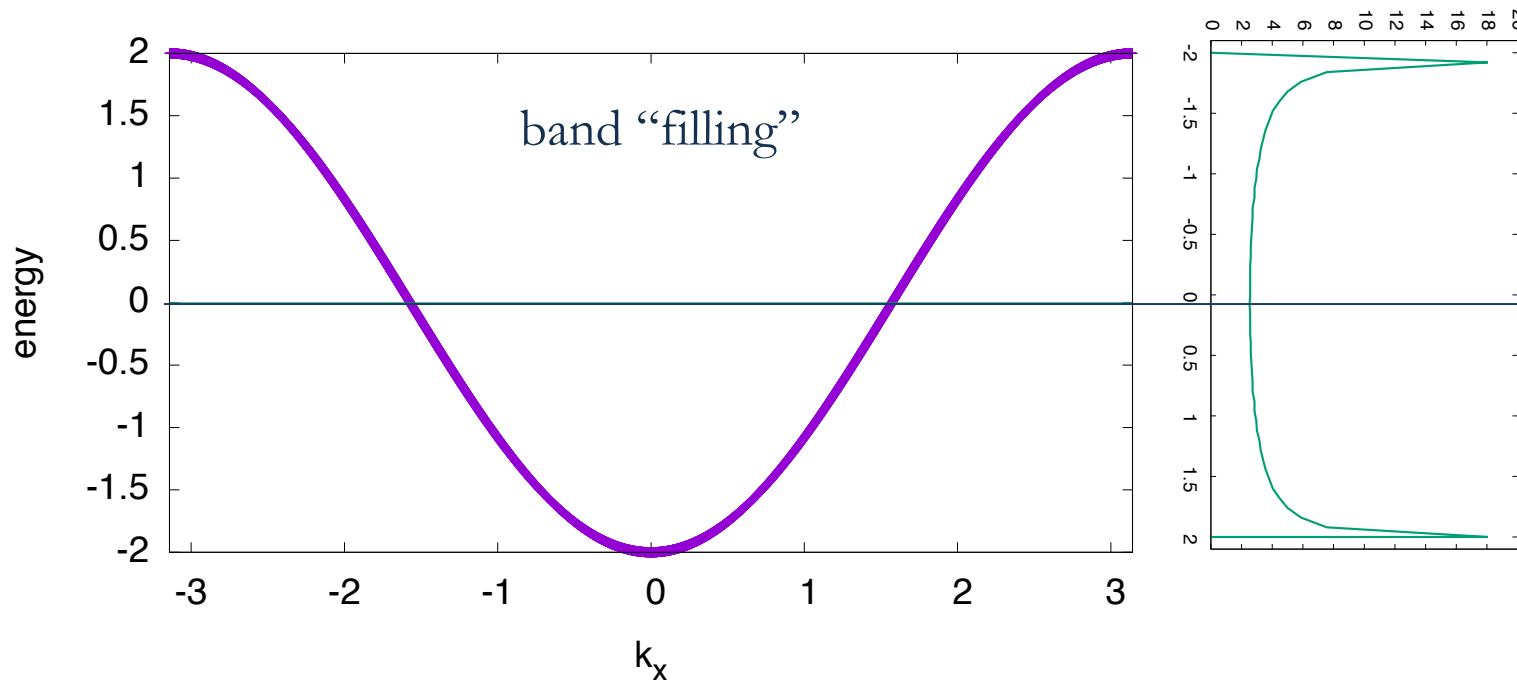
$$\psi(\mathbf{x}_1, \mathbf{x}_2) = \frac{1}{\sqrt{2}} [\phi_a(\mathbf{x}_1)\phi_b(\mathbf{x}_2) - \phi_b(\mathbf{x}_1)\phi_a(\mathbf{x}_2)]$$

Slater determinant

$$\psi(\mathbf{x}_1, \mathbf{x}_2, \dots, \mathbf{x}_N) = \frac{1}{\sqrt{N!}} \begin{vmatrix} \phi_{a_1}(\mathbf{x}_1) & \phi_{a_1}(\mathbf{x}_2) & \dots & \phi_{a_1}(\mathbf{x}_N) \\ \phi_{a_2}(\mathbf{x}_1) & \phi_{a_2}(\mathbf{x}_2) & \dots & \phi_{a_2}(\mathbf{x}_N) \\ \vdots & \vdots & \vdots & \vdots \\ \phi_{a_N}(\mathbf{x}_1) & \phi_{a_N}(\mathbf{x}_2) & \dots & \phi_{a_N}(\mathbf{x}_N) \end{vmatrix}$$

$$E = \sum_i \epsilon_{a_i}$$

Band “filling”, excitations, DOS



density of
states
(DOS)

$$N(\epsilon)$$

compressibility

$$\chi = N(\epsilon_F)$$

specific heat “Sommerfeld” coefficient

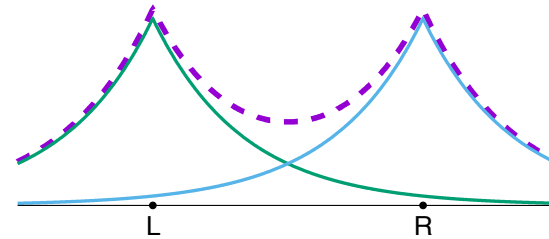
$$\gamma = \frac{\pi^2 k_B^2}{3} N(\epsilon_F)$$

$$C_V \sim \gamma T$$

Factorized wave function: a two-site example

$$\phi_a(\mathbf{x}) = c_{aL}\phi_L(\mathbf{x}) + c_{aR}\phi_R(\mathbf{x})$$

$$\phi_b(\mathbf{x}) = c_{bL}\phi_L(\mathbf{x}) + c_{bR}\phi_R(\mathbf{x})$$



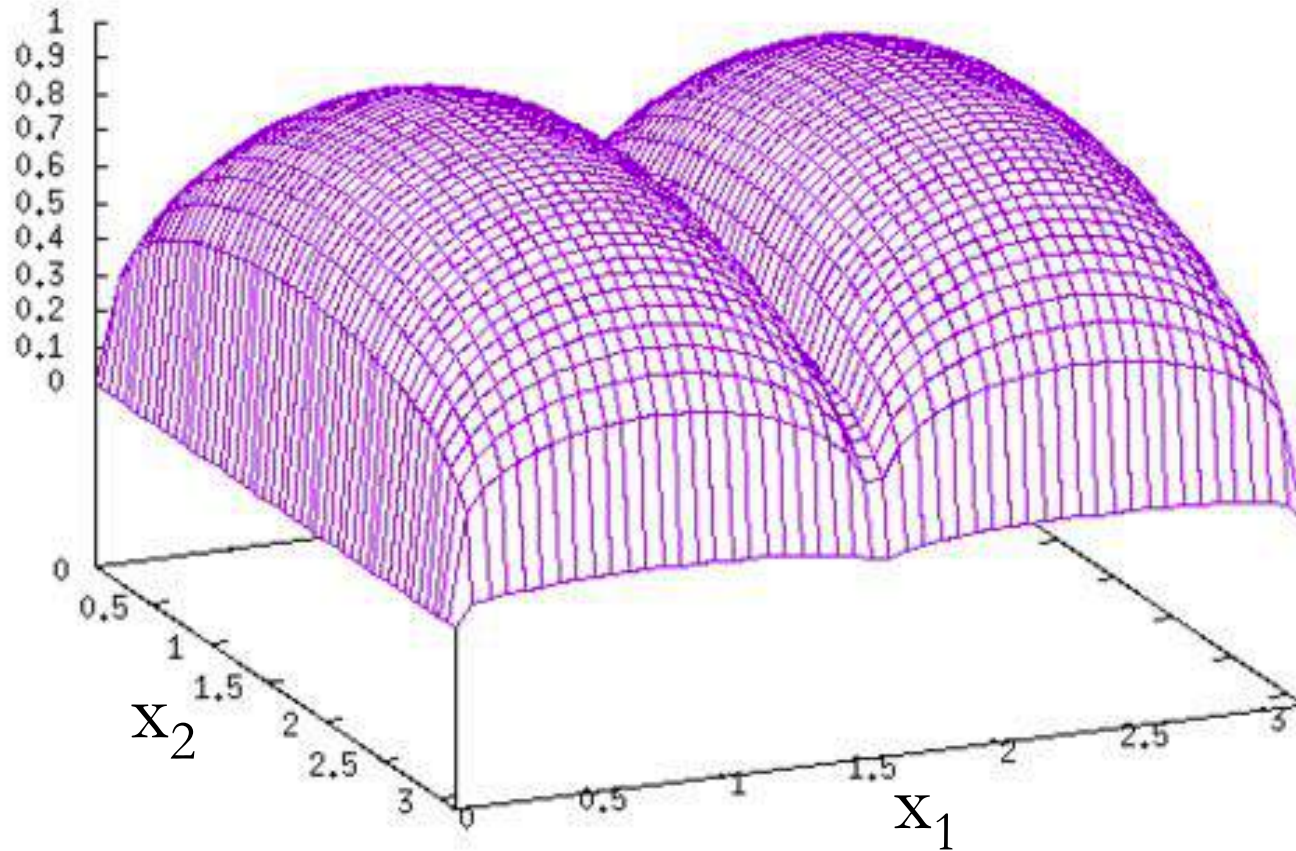
There is no way, by changing the one-electron wave functions (i.e. by changing c_{aL} , c_{aR} , c_{bL} and c_{bR}) to:

disfavour these contributions

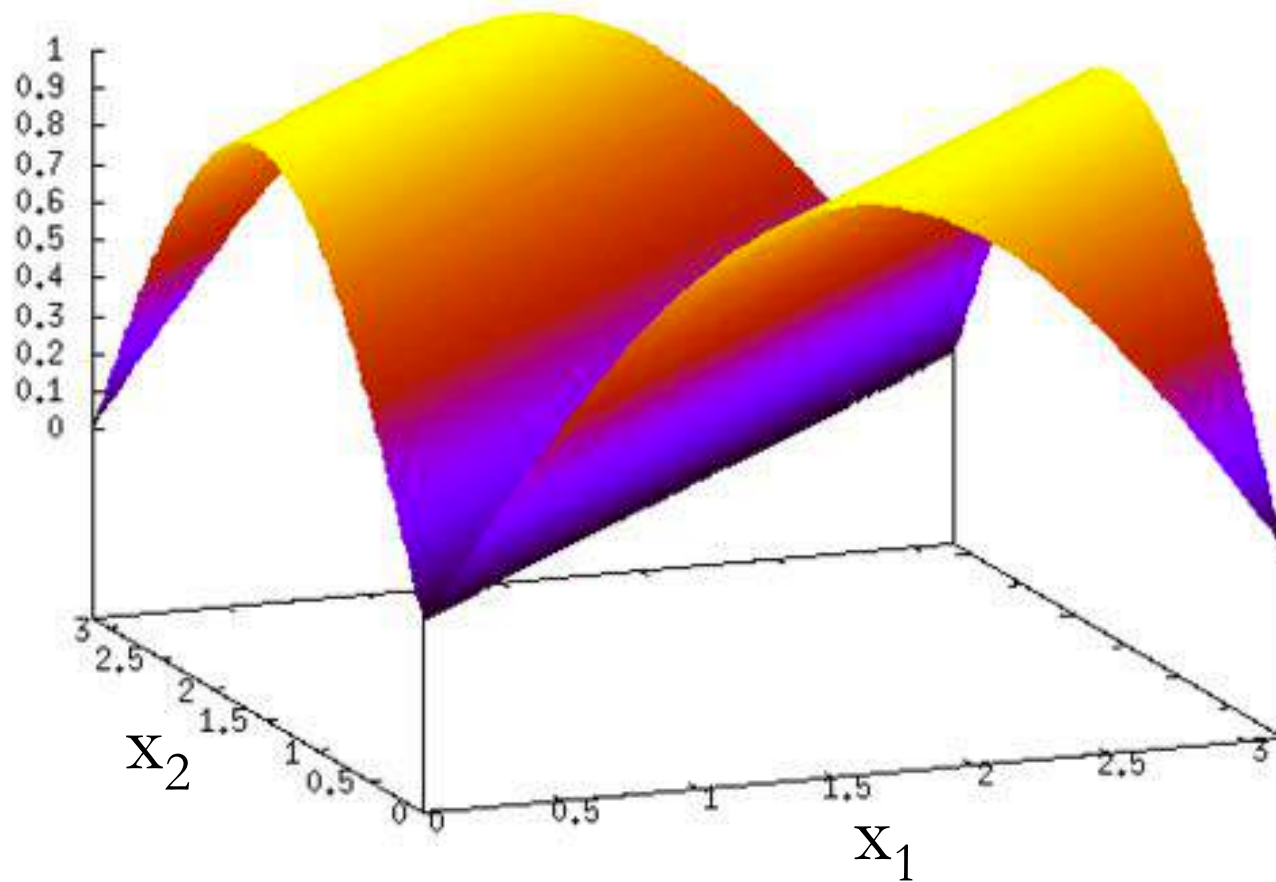
$$\begin{aligned} \phi_a(\mathbf{x}_1)\phi_b(\mathbf{x}_2) = & c_{aL}c_{bL}\phi_L(\mathbf{x}_1)\phi_L(\mathbf{x}_2) + c_{aR}c_{bR}\phi_R(\mathbf{x}_1)\phi_R(\mathbf{x}_2) \\ & + c_{aL}c_{bR}\phi_L(\mathbf{x}_1)\phi_R(\mathbf{x}_2) + c_{aR}c_{bL}\phi_R(\mathbf{x}_1)\phi_L(\mathbf{x}_2) \end{aligned}$$

favour these contributions

a factorized wave function



non-factorized wave function



orbital

single-orbital case

$$\hat{H} = \sum_{ij\sigma} t_{ij} d_{i\sigma}^\dagger d_{j\sigma} + U \sum_i \tilde{n}_{i\uparrow} \tilde{n}_{i\downarrow}$$

$$n_{im\sigma} = d_{im\sigma}^\dagger d_{im\sigma}$$

multi-orbital case

$$\hat{H} = \sum_{ijmm'\sigma} t_{ij}^{mm'} d_{im\sigma}^\dagger d_{jm'\sigma} + H_{int}$$

$$\tilde{n}_{m\sigma} \equiv n_{m\sigma} - 1/2$$

$$H_{int} = U \sum_m \tilde{n}_{m\uparrow} \tilde{n}_{m\downarrow} + (U - 2J) \sum_{m \neq m'} \tilde{n}_{m\uparrow} \tilde{n}_{m'\downarrow} + (U - 3J) \sum_{m < m', \sigma} \tilde{n}_{m\sigma} \tilde{n}_{m'\sigma}$$

Intra-orbital interaction

Inter-orbital interaction
 $U' < U$
for opposite spins

Inter-orbital interaction
 $U' - J < U' < U$
for parallel spins

J: “Hund’s coupling”

In correlated solids typically

$$J = 0.1 \div 0.2U$$

Hund's rules

Aufbau

	3d	4s
²¹ Sc	↑ □ □ □ □	↑↓
²² Ti	↑ ↑ □ □ □	↑↓
²³ V	↑ ↑ ↑ □ □	↑↓
²⁴ Cr	↑ ↑ ↑ ↑ ↑	↑
²⁵ Mn	↑ ↑ ↑ ↑ ↑	↑↓
²⁶ Fe	↑↓ ↑ ↑ ↑ ↑	↑↓
²⁷ Co	↑↓ ↑↓ ↑ ↑ ↑	↑↓
²⁸ Ni	↑↓ ↑↓ ↑↓ ↑ ↑	↑↓
²⁹ Cu	↑↓ ↑↓ ↑↓ ↑↓ ↑	↑
³⁰ Zn	↑↓ ↑↓ ↑↓ ↑↓ ↑↓	↑↓

Hund's Rules

In open shells:

1. Maximize total spin S
2. Maximize total angular momentum T
- (3. Dependence on $J=T+S$, Spin-orbit effects)

Slave-spin mean field

Slave variables mean fields (general)

Recipe:

- Enlarge the local Hilbert space (new variables + constraint)
- Decouple the pseudo-fermions from the slave variables (renormalized non-interacting fermionic model)
- Treat the slave variables in a local mean-field
- Treat the constraint on average

Examples:

- Slave Bosons (Coleman, PRB 29, 3035 (1984) - Kotliar and Ruckenstein, PRL 57, 1362 (1987))
- Slave Rotors (Florens and Georges, PRB70, 035114 (2004))

Slave-spins

de' Medici et al. PRB 72, 205124 (2005)

S. R. Hassan and LdM, PRB 81, 35106 (2010)

Hilbert Space mapping:

$$|n_{i\sigma}^d = 1\rangle \iff |n_{i\sigma}^f = 1, S_{i\sigma}^z = +1/2\rangle$$

$$|n_{i\sigma}^d = 0\rangle \iff |n_{i\sigma}^f = 0, S_{i\sigma}^z = -1/2\rangle$$

$$f_{i\sigma}^\dagger f_{i\sigma} = S_{i\sigma}^z + \frac{1}{2}$$

constraint,
to exclude unphysical states

Slave-spin mean field

The density-density interactions are easily re-expressed through slave-spin operators

$$n_{i\sigma}^d \iff n_{i\sigma}^f$$

$$n_{i\sigma}^d \iff S_{i\sigma}^z + \frac{1}{2}$$

$$(\tilde{n}_{m\sigma} \equiv n_{m\sigma} - 1/2)$$

$$H_{int} = U \sum_m \tilde{n}_{m\uparrow} \tilde{n}_{m\downarrow} + (U - 2J) \sum_{m \neq m'} \tilde{n}_{m\uparrow} \tilde{n}_{m'\downarrow} + (U - 3J) \sum_{m < m', \sigma} \tilde{n}_{m\sigma} \tilde{n}_{m'\sigma}$$

$$H_{int}[S] = U \sum_m S_{m\uparrow}^z S_{m\downarrow}^z + (U - 2J) \sum_{m \neq m'} S_{m\uparrow}^z \tilde{S}_{m'\downarrow}^z + (U - 3J) \sum_{m < m', \sigma} S_{m\sigma}^z S_{m'\sigma}^z$$

Hopping terms

$$d_{i\sigma} \rightarrow f_{i\sigma} O_{i\sigma}$$

$$O_{m\sigma} = S_{m\sigma}^- + c_{m\sigma} S_{m\sigma}^+$$

$$c_m = \frac{1}{\sqrt{\langle n_{m\sigma}^f \rangle (1 - \langle n_{m\sigma}^f \rangle)}} - 1$$

$$d_{i\sigma}^\dagger \rightarrow f_{i\sigma}^\dagger O_{i\sigma}^\dagger$$

in the constrained space

$$H - \mu \hat{N} = \sum_{i \neq j, \sigma} t_{ij}^{mm'} O_{im\sigma}^\dagger O_{jm'\sigma} f_{im\sigma}^\dagger f_{jm'\sigma} + \sum_{im\sigma} (\epsilon_m - \mu) n_{im\sigma}^f + H_{int}[S]$$

Slave-spin mean field

Finally: mean-field equations (constraint treated on average: lagrange multipliers λ_m)

$$H_f = \sum_{i \neq j, mm' \sigma} t_{ij}^{mm'} \sqrt{Z_m Z_{m'}} f_{im\sigma}^\dagger f_{jm'\sigma} + \sum_{im\sigma} (\epsilon_m - \lambda_m - \mu) n_{im\sigma}^f,$$

$$H_s = \sum_{m, \sigma} \left[(h_m O_{m\sigma}^\dagger + H.c.) + \lambda_m (S_{m\sigma}^z + \frac{1}{2}) \right] + \hat{H}_{int}[S],$$

$$h_{m\sigma} = \sum_{m'} \langle O_{m'\sigma} \rangle_s \sum_{j(\neq i)} t_{ij}^{mm'} \langle f_{im\sigma}^\dagger f_{jm'\sigma} \rangle_f$$

$$Z_m = |\langle O_{m\sigma} \rangle|^2 \qquad \langle S_{i\sigma}^z \rangle + \frac{1}{2} = \langle f_{i\sigma}^\dagger f_{i\sigma} \rangle$$

Analogous to multi-orbital Kotliar-Ruckenstein slave-bosons and Gutzwiller approximation (F. Gebhard lecture)

Similarly, the Slave-spin mean-field (SSMF) describes a Fermi-liquid

Pedagogical introduction:

"Modeling Many-Body Physics with Slave-Spin Mean-Field : Mott and Hund's Physics in Fe-Superconductors", L. de' Medici and M. Capone in *The Iron Pnictide Superconductors*, Springer Series in Solid-State Sciences, Vol. 186, pp. 115-185, Mancini, F., Citro, R. (Eds) 2017.

Fermi Liquid Theory

quasiparticles instead of particles

$$\frac{1}{\tau} = a(\epsilon - \epsilon_F)^2 + bT^2 \quad \text{infinite lifetime at } T=0 \text{ at the Fermi level}$$

$$\epsilon_{n\mathbf{k}} \longrightarrow \epsilon_{n\mathbf{k}}^* \quad \text{renormalized dispersion}$$

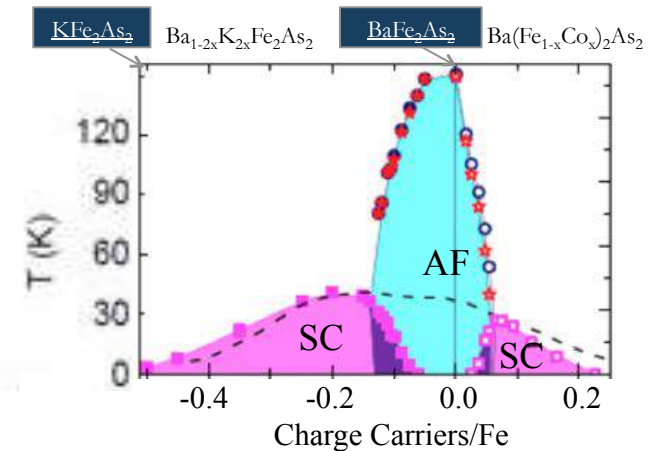
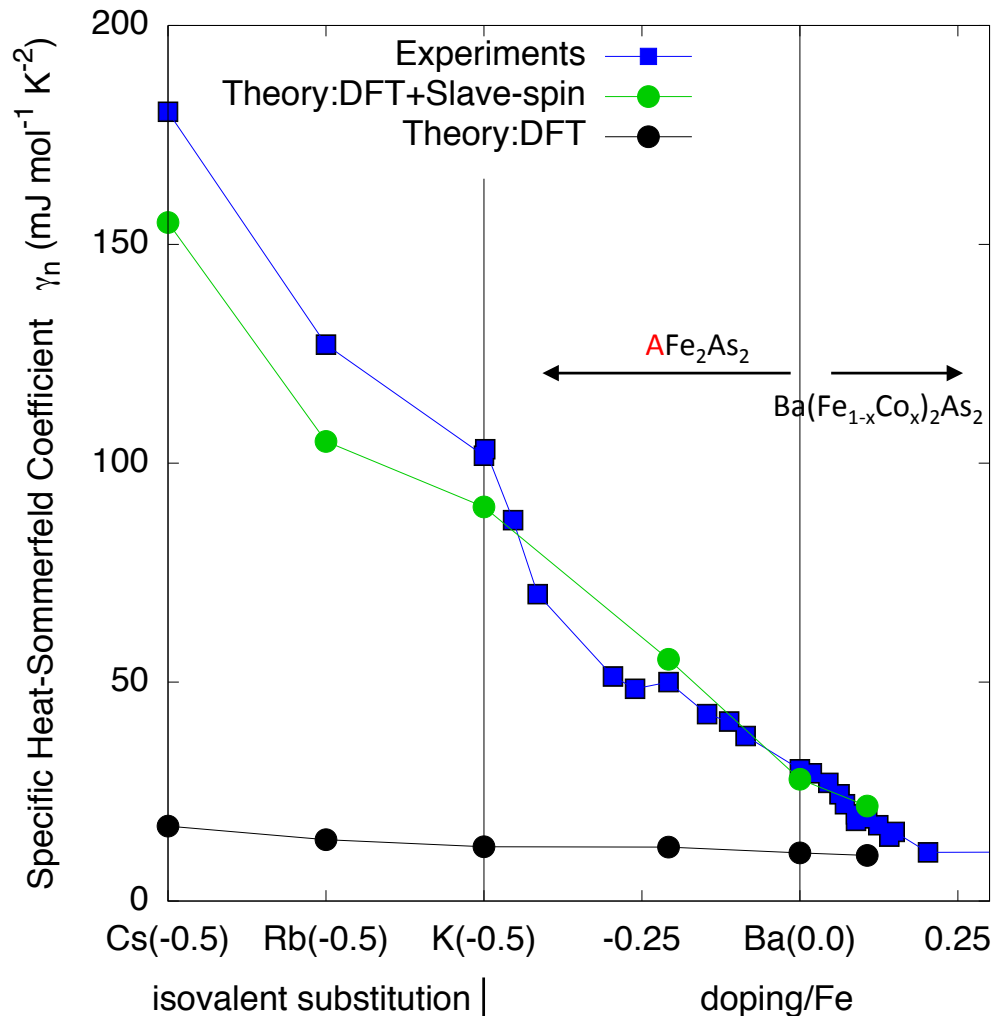
$$N(\epsilon_F) \longrightarrow N^*(\epsilon_F) \quad \text{renormalized DOS}$$

$$\mathbf{v}_{n\mathbf{k}}^* = \frac{1}{\hbar} \nabla_{\mathbf{k}} \epsilon_{n\mathbf{k}}^* \quad |\mathbf{v}_{n\mathbf{k}}^*| = \frac{\hbar k}{m^*} \quad \text{effective mass}$$

$$\chi = \frac{N^*(\epsilon_F)}{1 + F_0^s} \quad \text{compressibility}$$

$$\gamma = \frac{\pi^2 k_B^2}{3} N^*(\epsilon_F) \quad \text{Sommerfeld coefficient}$$

Fe-superconductors: specific heat



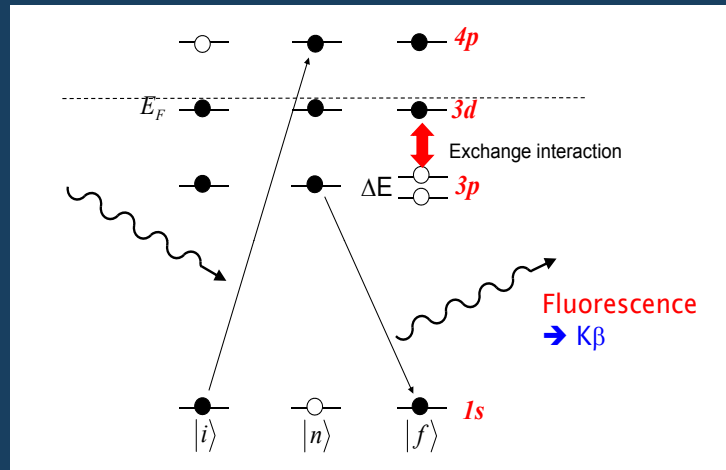
Theory (DFT+Slave-spin):

- the same interaction parameters ($U=2.7\text{eV}$, $J/U=0.25$) capture the whole material trend
- DFT results are completely off: strong correlations

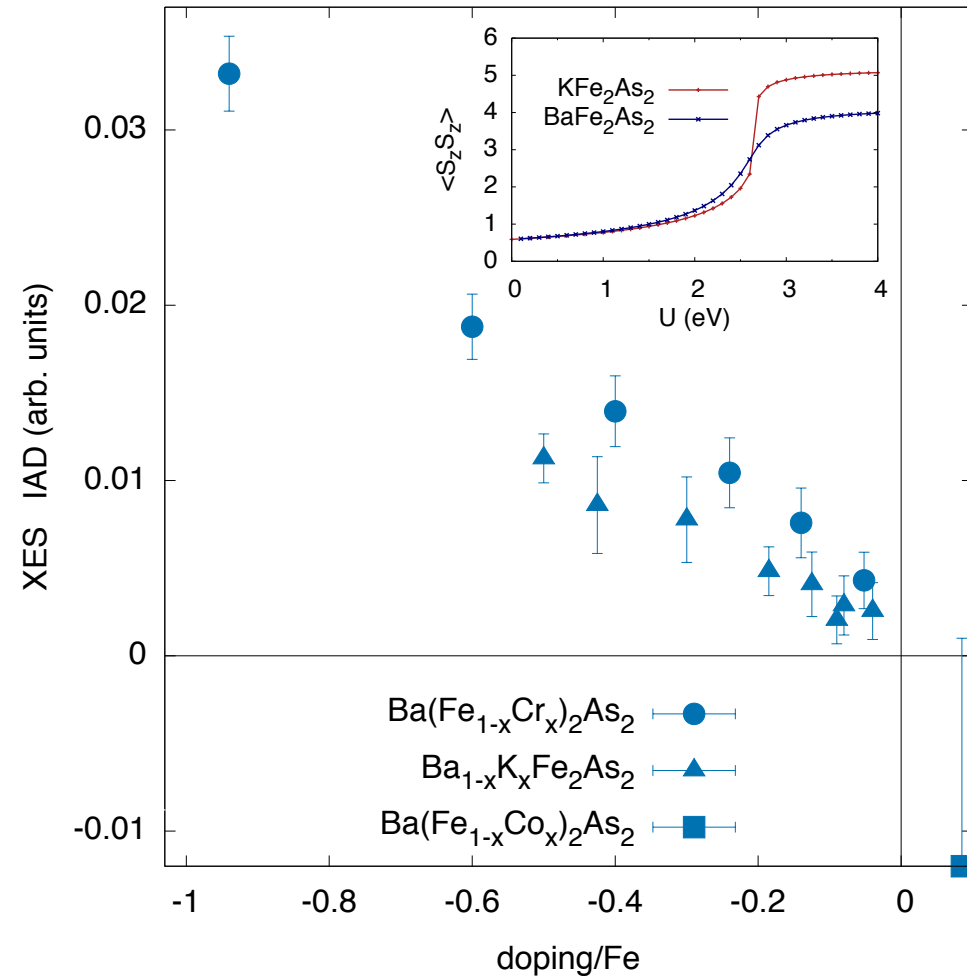
Experiments: C. Meingast's group in Karlsruhe. F. Hardy, ..., LdM et al. PRB 94, 205113 (2016)

Fe-superconductors: local moments

X-ray Emission Spectroscopy (K- β / β' line shift)



© Young-June Kim (U Toronto)



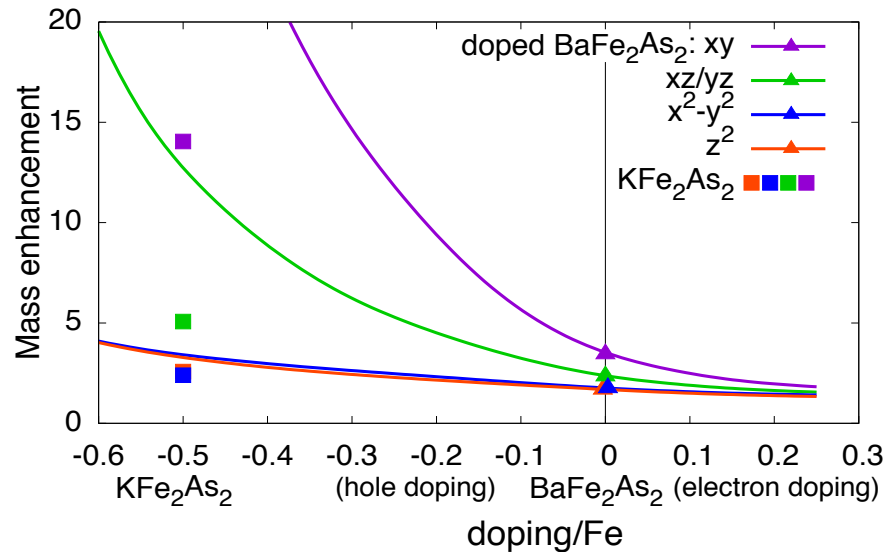
P. Glatzel group @ ESRF (ID26)

S. Lafuerza, ..., LdM et al., PRB 96, 045133 (2017)

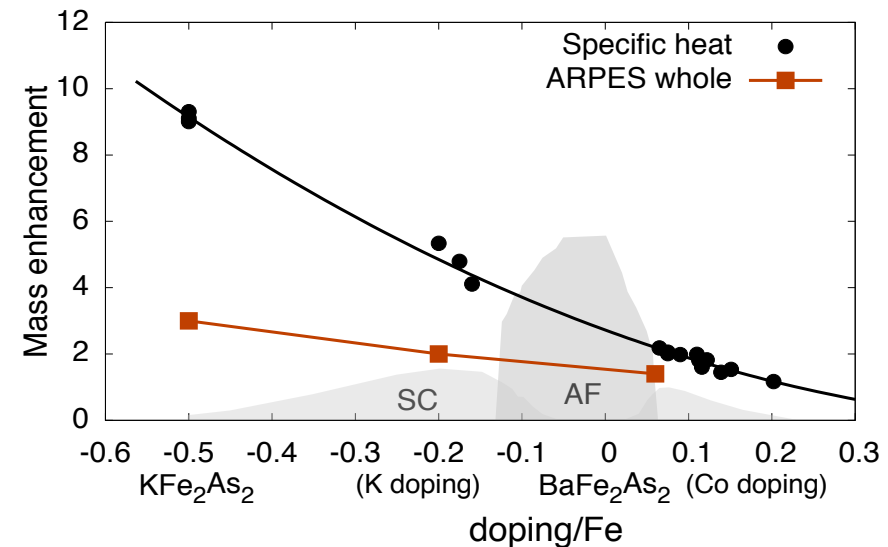
see also Pellicciari et al. Sci. Rep. 7, 8003 (2017)

Fe-superconductors: orbital-selectivity

Theory (LDA+Slave-spins)



Experimental data
(high-T tetragonal phase)



LdM, Giovannetti, Capone, PRL 2014 “Selective Mott Physics as a Key to Iron Superconductors”

Selective correlation strength:
strongly *and* weakly correlated electrons coexisting

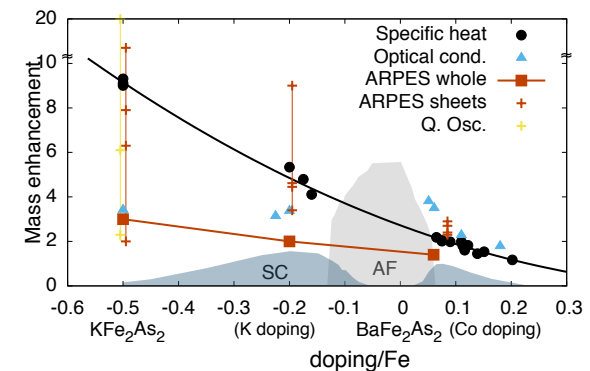
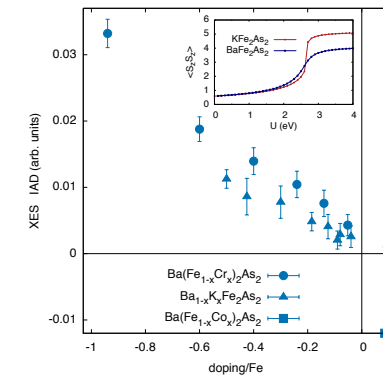
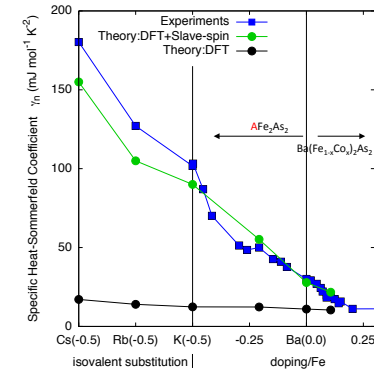
LdM, *Weak AND strong correlations in Fe-SC*, in “Iron-based Superconductivity”, Springer book 2015

Hund's metals

3 main features:

- enhanced electron correlations and masses
- high local spin configurations dominating the paramagnetic fluctuations
- orbital-selectivity of the electron correlation strength

which are due to the proximity to a **Hund's favored** Mott insulating state for half-filled conduction bands (1 hole/Fe doping)

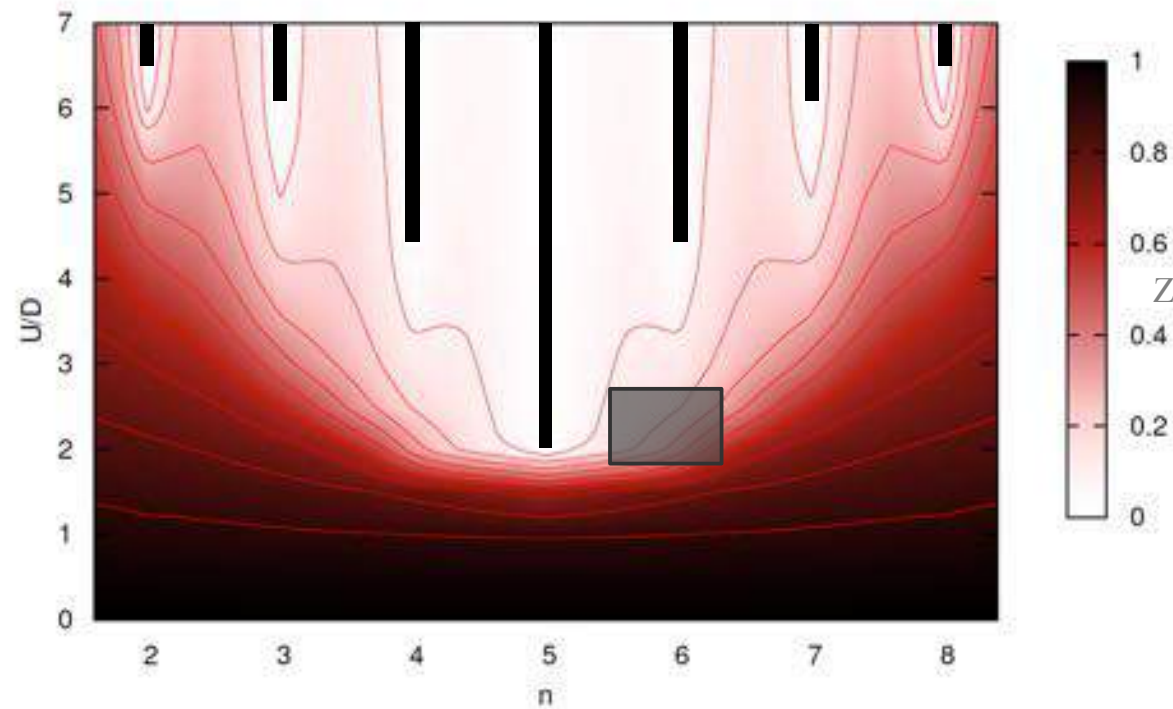


5-orbital Hubbard model

$J/U=0.15$

$J/U=0.20$

$J/U=0.25$



Semicircular DOS of width $W=2D$
(Bethe lattice with hopping t , $D=2t$)

$$D(\epsilon) = \frac{2}{\pi D} \sqrt{1 - \frac{\epsilon^2}{D^2}}$$

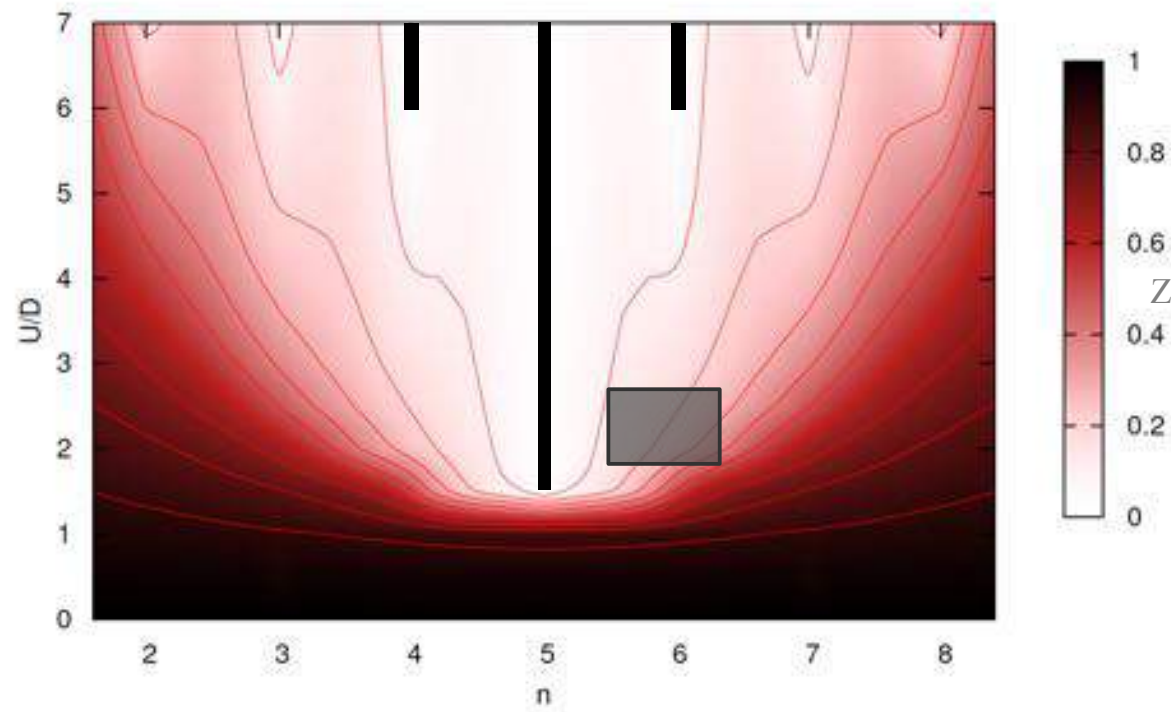
LdM, *Weak AND strong correlations in Fe Superconductors*, in “Iron-based Superconductivity”, Springer Series in Material Sciences, Vol 211, pp 409-441 (2015) - ArXiv: 1506.01678

5-orbital Hubbard model

$J/U=0.15$

$J/U=0.20$

$J/U=0.25$



Semicircular DOS of width $W=2D$
(Bethe lattice with hopping t , $D=2t$)

$$D(\epsilon) = \frac{2}{\pi D} \sqrt{1 - \frac{\epsilon^2}{D^2}}$$

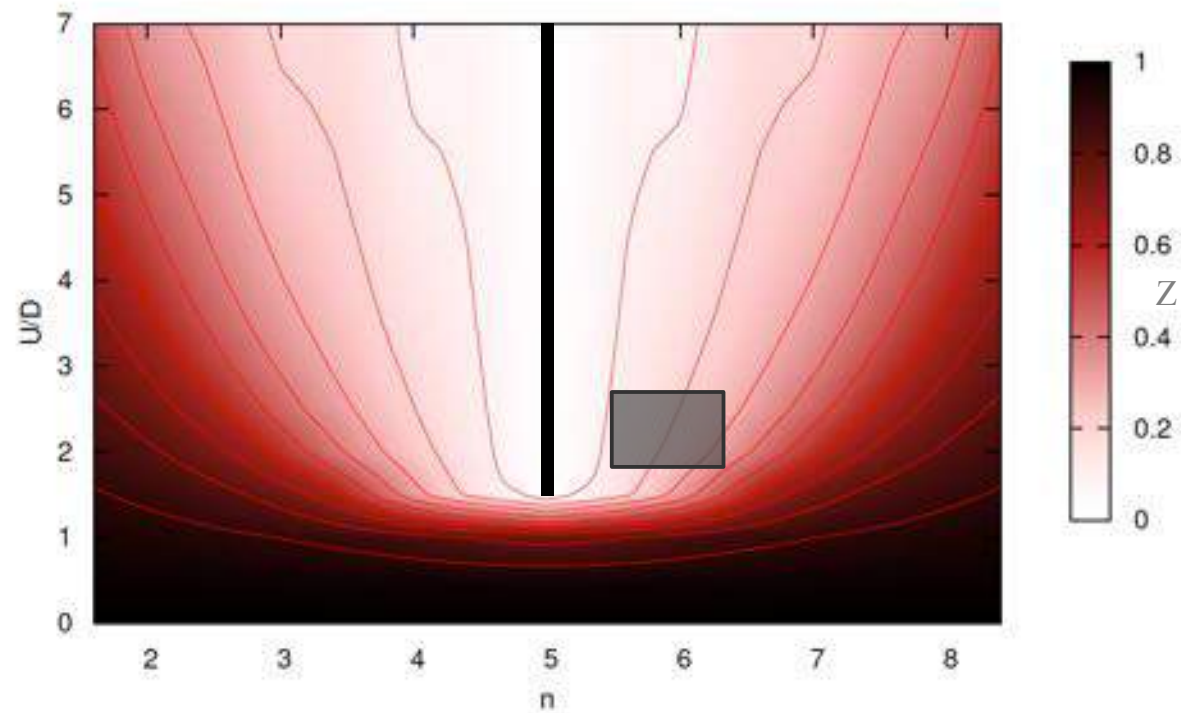
LdM, *Weak AND strong correlations in Fe Superconductors*, in “Iron-based Superconductivity”,
Springer Series in Material Sciences, Vol 211, pp 409-441 (2015) - ArXiv: 1506.01678

5-orbital Hubbard model

$J/U=0.15$

$J/U=0.20$

$J/U=0.25$



Semicircular DOS of width $W=2D$
(Bethe lattice with hopping t , $D=2t$)

$$D(\epsilon) = \frac{2}{\pi D} \sqrt{1 - \frac{\epsilon^2}{D^2}}$$

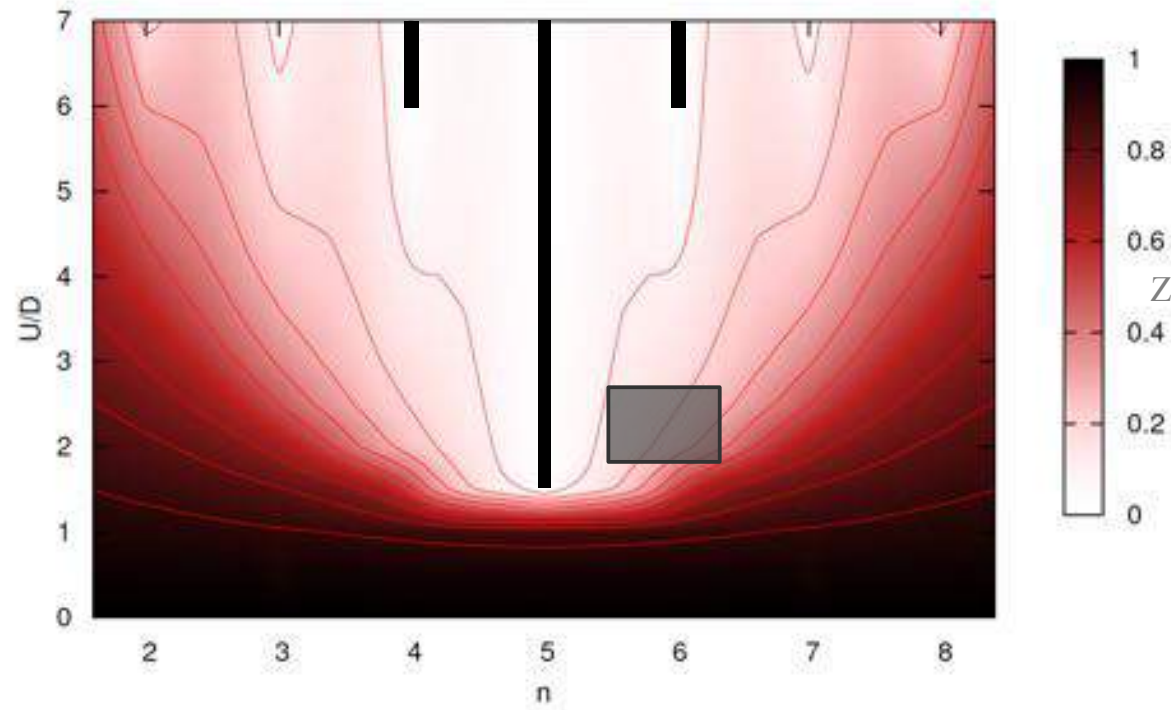
LdM, *Weak AND strong correlations in Fe Superconductors*, in “Iron-based Superconductivity”, Springer Series in Material Sciences, Vol 211, pp 409-441 (2015) - ArXiv: 1506.01678

5-orbital Hubbard model

$J/U=0.15$

$J/U=0.20$

$J/U=0.25$



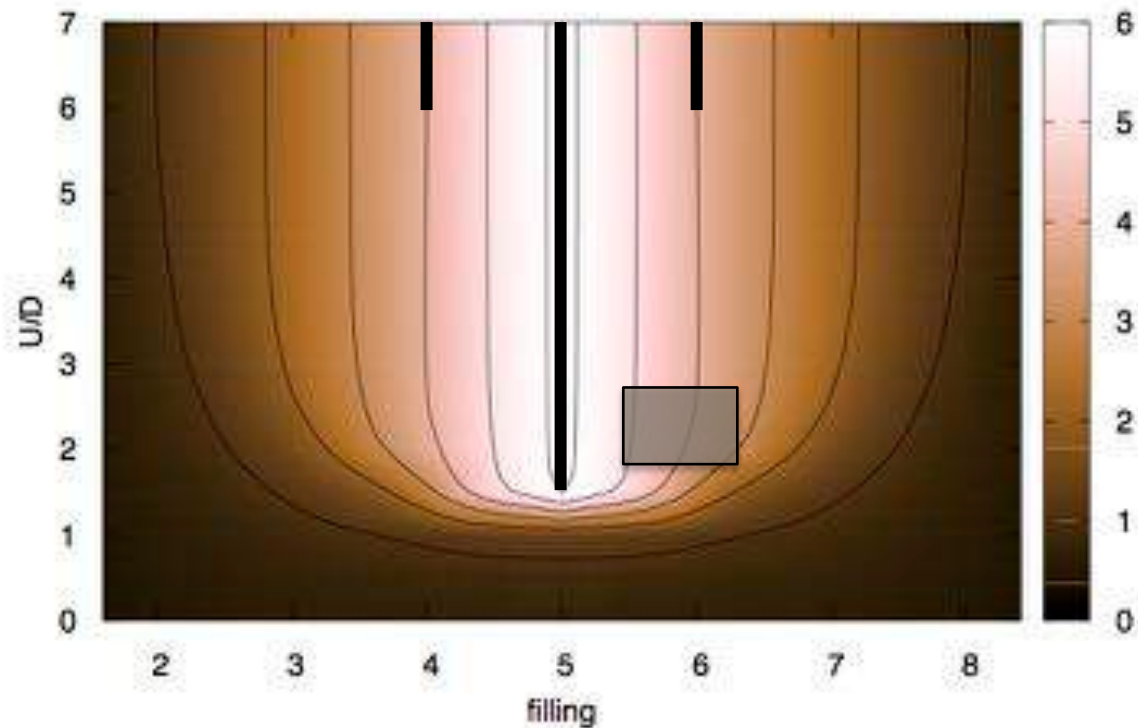
Semicircular DOS of width $W=2D$
(Bethe lattice with hopping t , $D=2t$)

$$D(\epsilon) = \frac{2}{\pi D} \sqrt{1 - \frac{\epsilon^2}{D^2}}$$

LdM, *Weak AND strong correlations in Fe Superconductors*, in “Iron-based Superconductivity”, Springer Series in Material Sciences, Vol 211, pp 409-441 (2015) - ArXiv: 1506.01678

High fluctuating magnetic moment

$$J/U=0.20$$

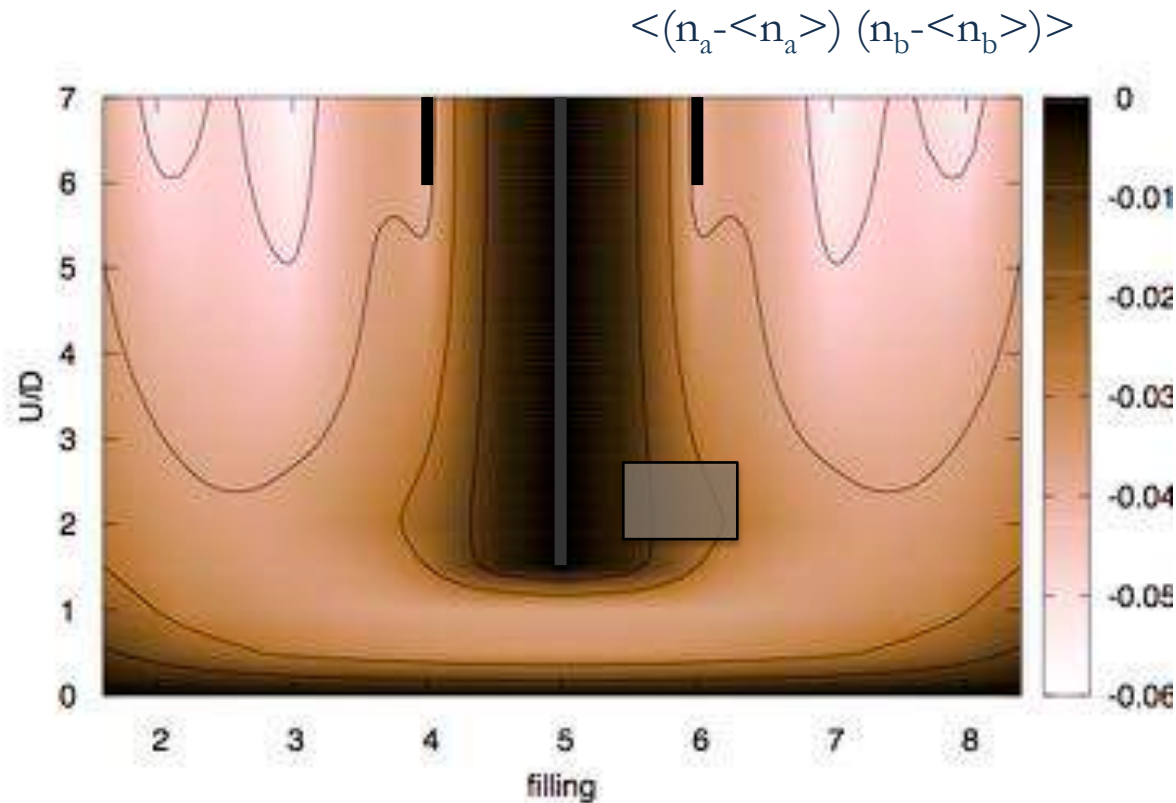


A metal in which high-spin configurations prevail

“Hund’s metal”

inter-orbital charge correlations

$$J/U=0.20$$



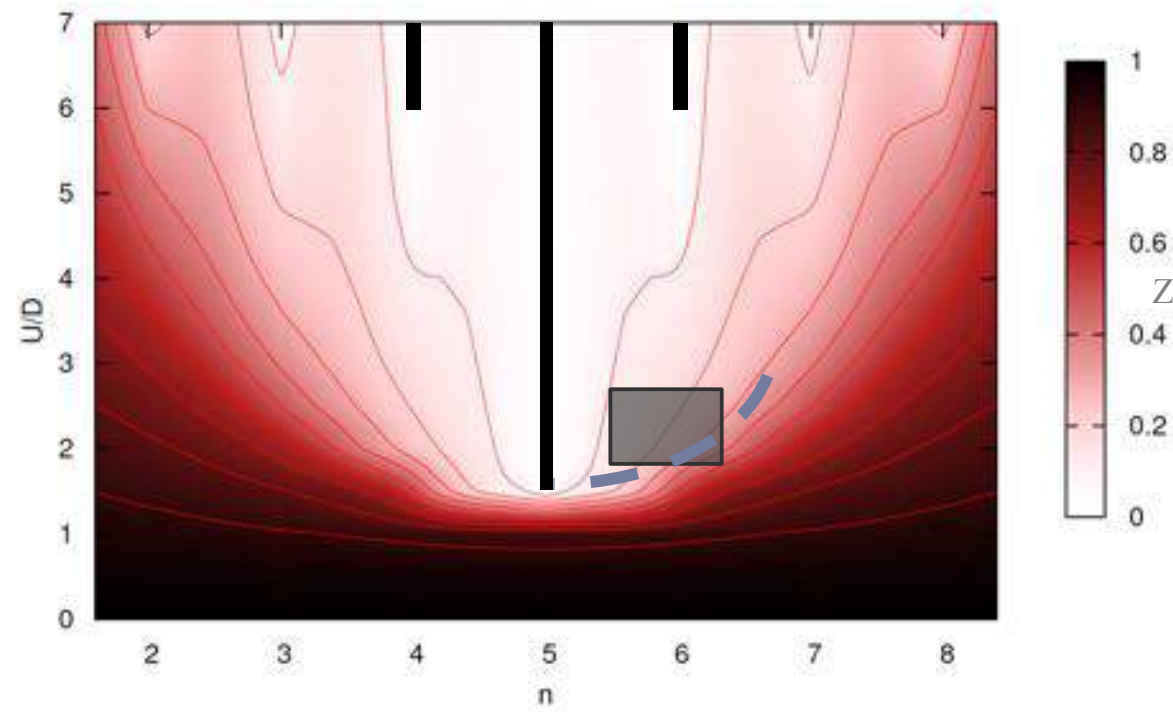
charge fluctuations in different orbitals become uncorrelated near the half-filled Mott insulator

Hund's metal and half-filled Mott insulator

$J/U=0.15$

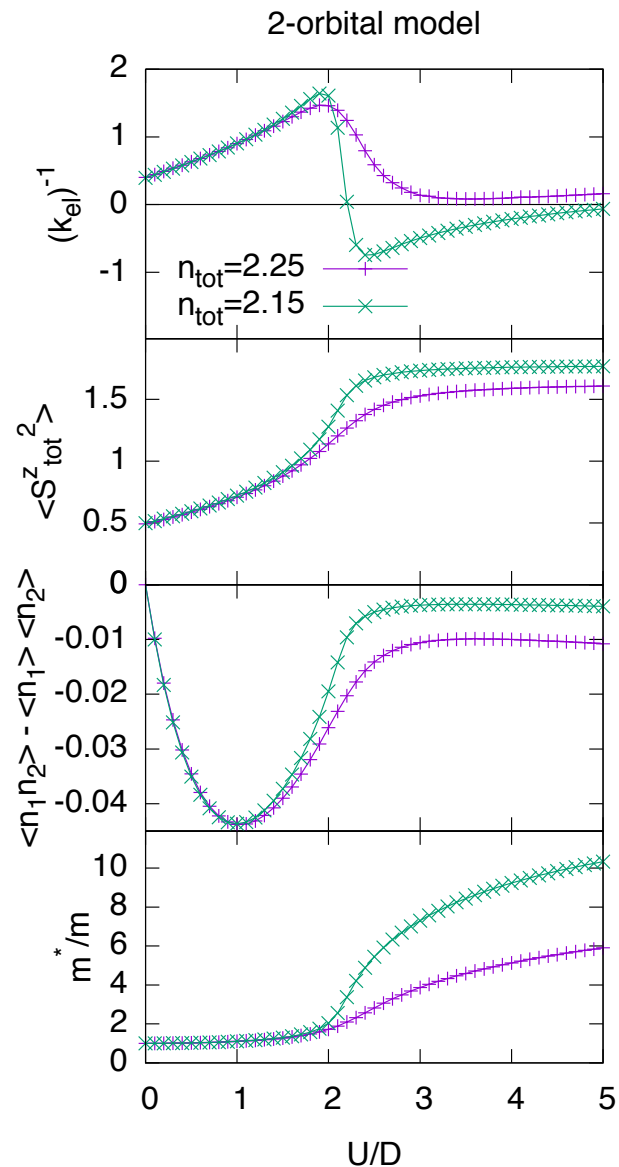
$J/U=0.20$

$J/U=0.25$

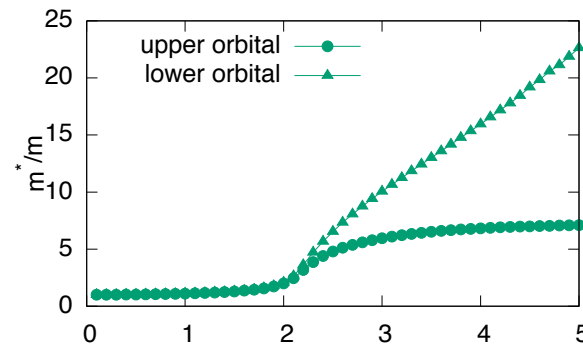


The cross-over departs from the Mott transition
at half-filling

Hund's metal frontier: 2-orbital Hubbard model



$J/U=0.25$



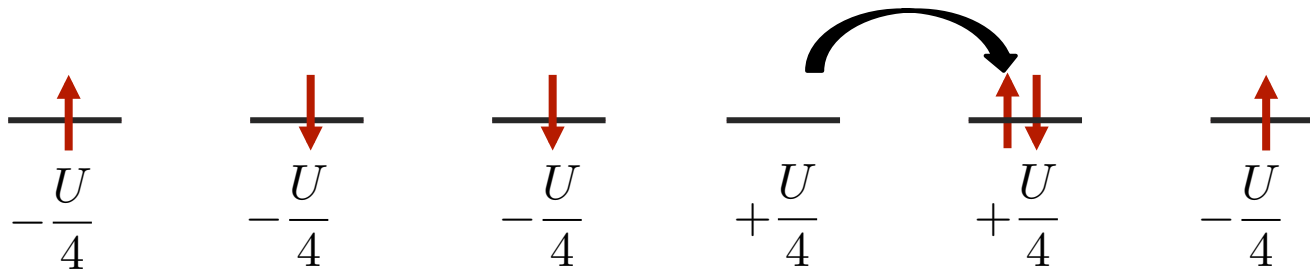
2-orbital case $n_{tot}=2.15$,
with a small crystal-field
splitting $\epsilon_1 - \epsilon_2 = 0.05D$

Hund's phenomenology analogous
to the 5-orbital (and 3-orbital) case
and to the realistic simulations for
the Fe-superconductors: generic

Mott transition: the atomic Mott gap

Single band Hubbard model
in the atomic limit

$$\sum_i U \left(n_{i\uparrow} - \frac{1}{2} \right) \left(n_{i\downarrow} - \frac{1}{2} \right)$$



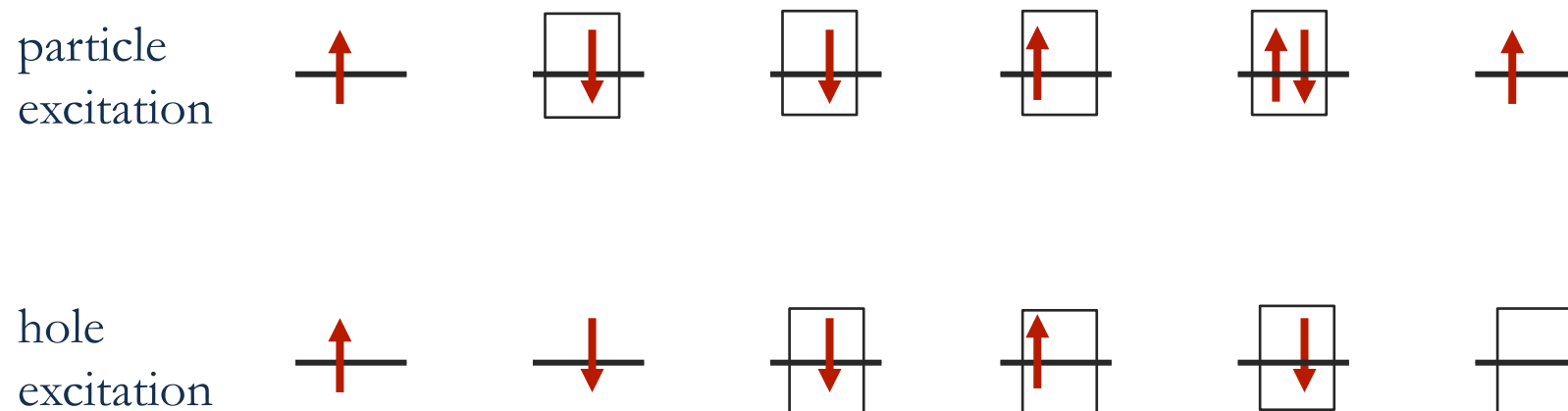
Potential energy barrier to overcome to establish conduction
(ionization energy - electron affinity)

$$\begin{aligned} \Delta_{at} &= E_{at}(n+1) - E_{at}(n) + E_{at}(n-1) - E_{at}(n) \\ &= E_{at}(n+1) + E_{at}(n-1) - 2E_{at}(n) \end{aligned}$$

$$\Delta_{at} = U$$

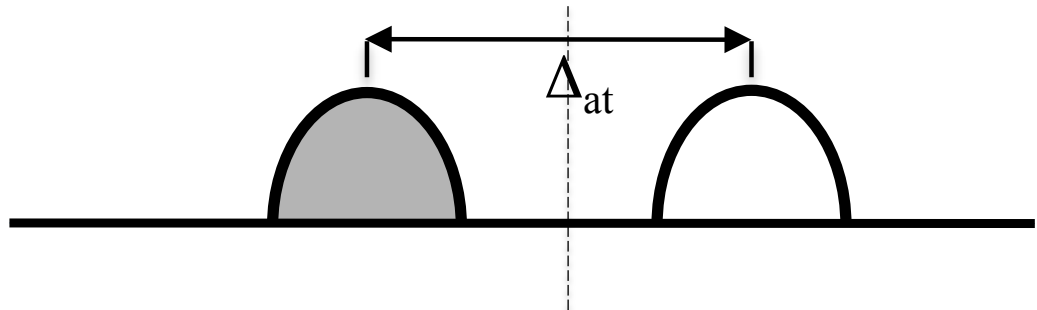
Mott transition: Hubbard bands

However these excited states are mobile
(high degeneracy removed by hopping \rightarrow energy dispersion $\sim W$)

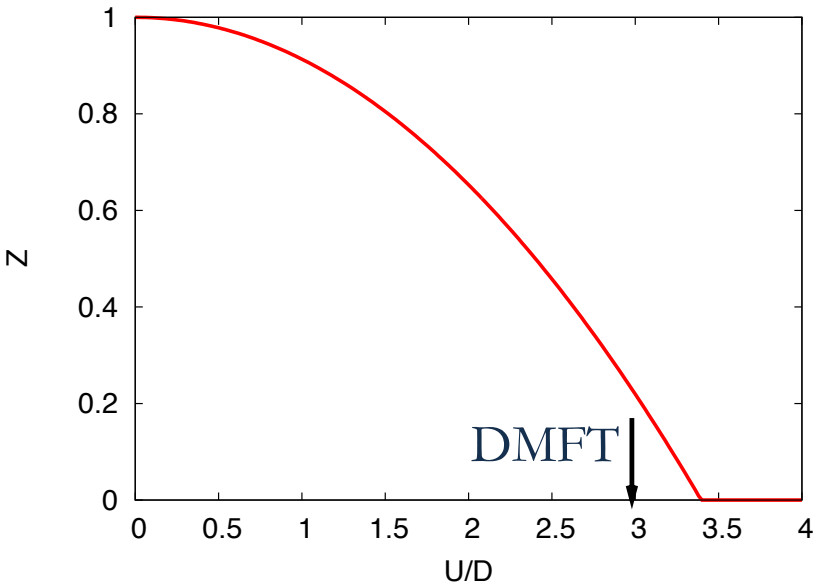


Formation of two “Hubbard bands” in the spectrum of excitations

Mott transition: the Hubbard criterion



$$\Delta = U - W \quad \longrightarrow \quad U_c = W$$



Slave-spin mean-field
half-filled 1-band Hubbard model
Semi-circular Density of states
of width $W=2D$

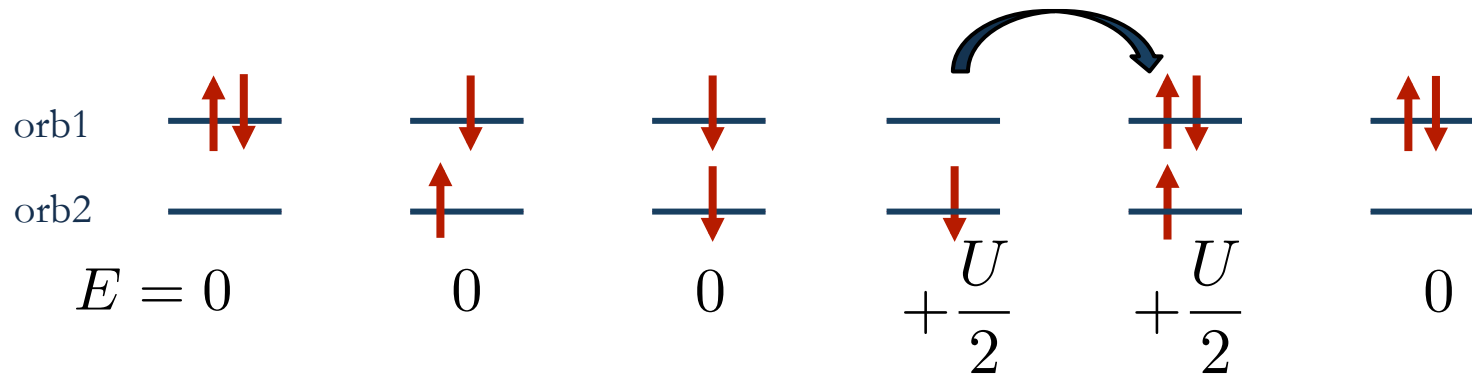
The gap for Hund's metal interaction at $J=0$

At $J=0$, the interaction is proportional to the total charge on the site squared

$$H_{int} = \sum_i \frac{U}{2} \left(\sum_{m\sigma} (n_{im\sigma} - \frac{1}{2}) \right)^2 = \sum_i \frac{U}{2} (n_i^{tot} - M)^2$$

M number of orbitals

all configurations with the same number of electrons on a site have the same interaction energy.



$$\Delta_{at} = E_{at}(n + 1) + E_{at}(n - 1) - 2E_{at}(n)$$

The atomic potential barrier is still U

$$\Delta_{at} = U$$

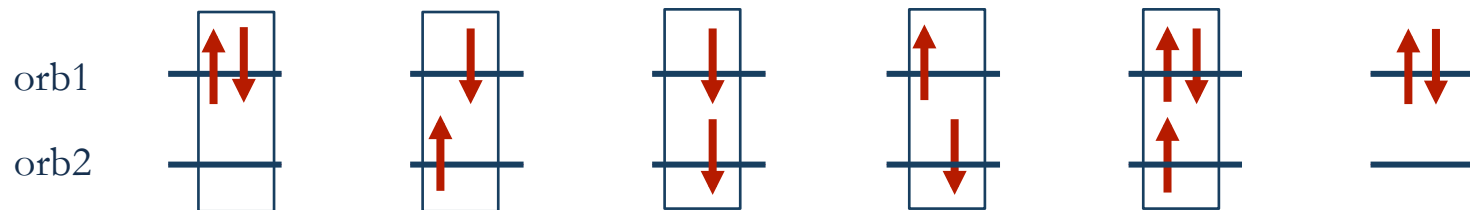
Hubbard bands at $J=0$

At $J=0$, the interaction is proportional to the total charge on the site

$$H_{int} = \sum_i \frac{U}{2} \left(\sum_{m\sigma} (n_{im\sigma} - \frac{1}{2}) \right)^2 = \sum_i \frac{U}{2} (n_i^{tot} - M)^2$$

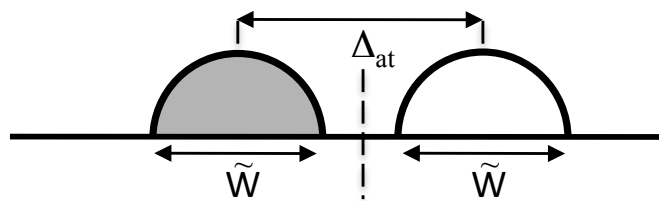
M number of orbitals

all configurations with the same number of electrons on a site have the same interaction energy.



More hopping channels, larger degeneracy-removal energy

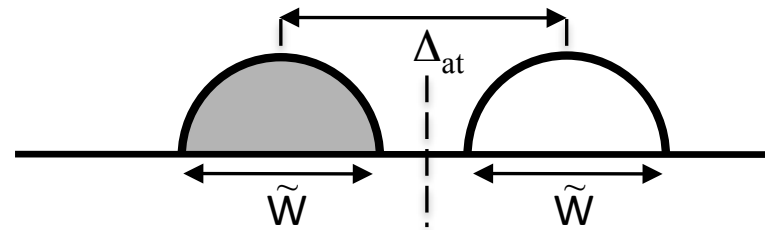
Wider Hubbard bands



$$\tilde{W} = \sqrt{M} W$$

Gunnarsson et al.
PRB 56, 1146 (1997)

Mott transition in multi-orbital models

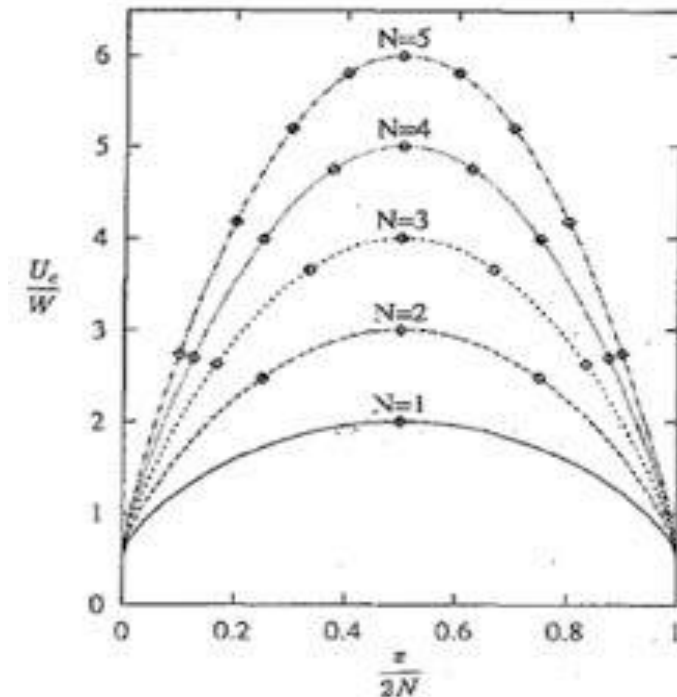


N orbitals

$$\Delta = U - \tilde{W} \quad \longrightarrow \quad U_c = \tilde{W} = \sqrt{M} W$$

Mott transitions at $J=0$

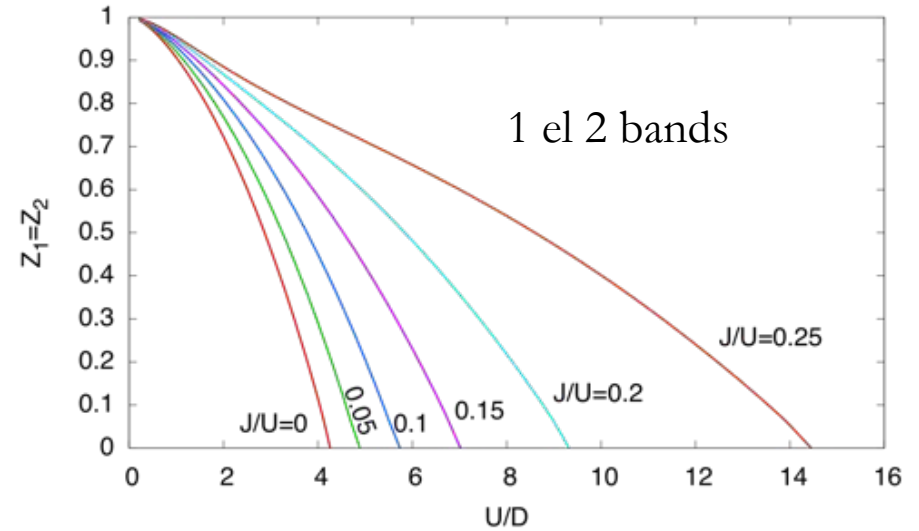
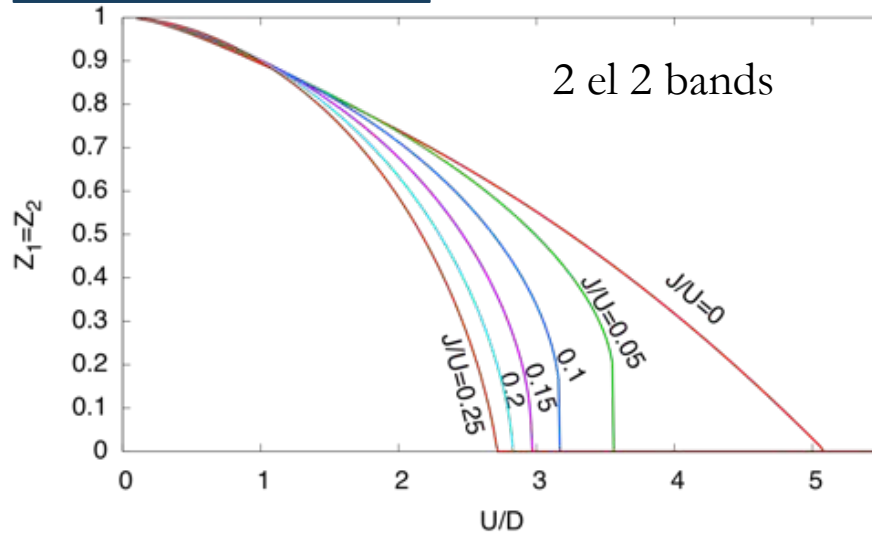
- Mott transition at every integer filling, U_c grows with M
- U_c is maximum at half-filling



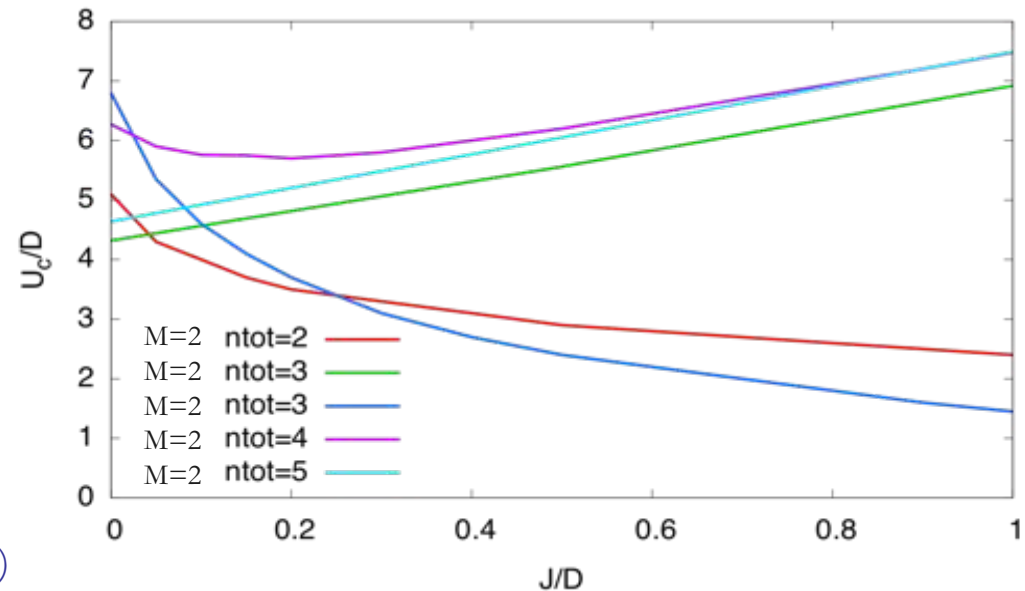
M-orbital degenerate Hubbard model: Slave-spins

effect of Hund's J

Quasiparticle renormalization factor $Z=(m^*/m)^{-1}$



U_c is lowered by J
only for half-filling.
In all other cases is
enhanced

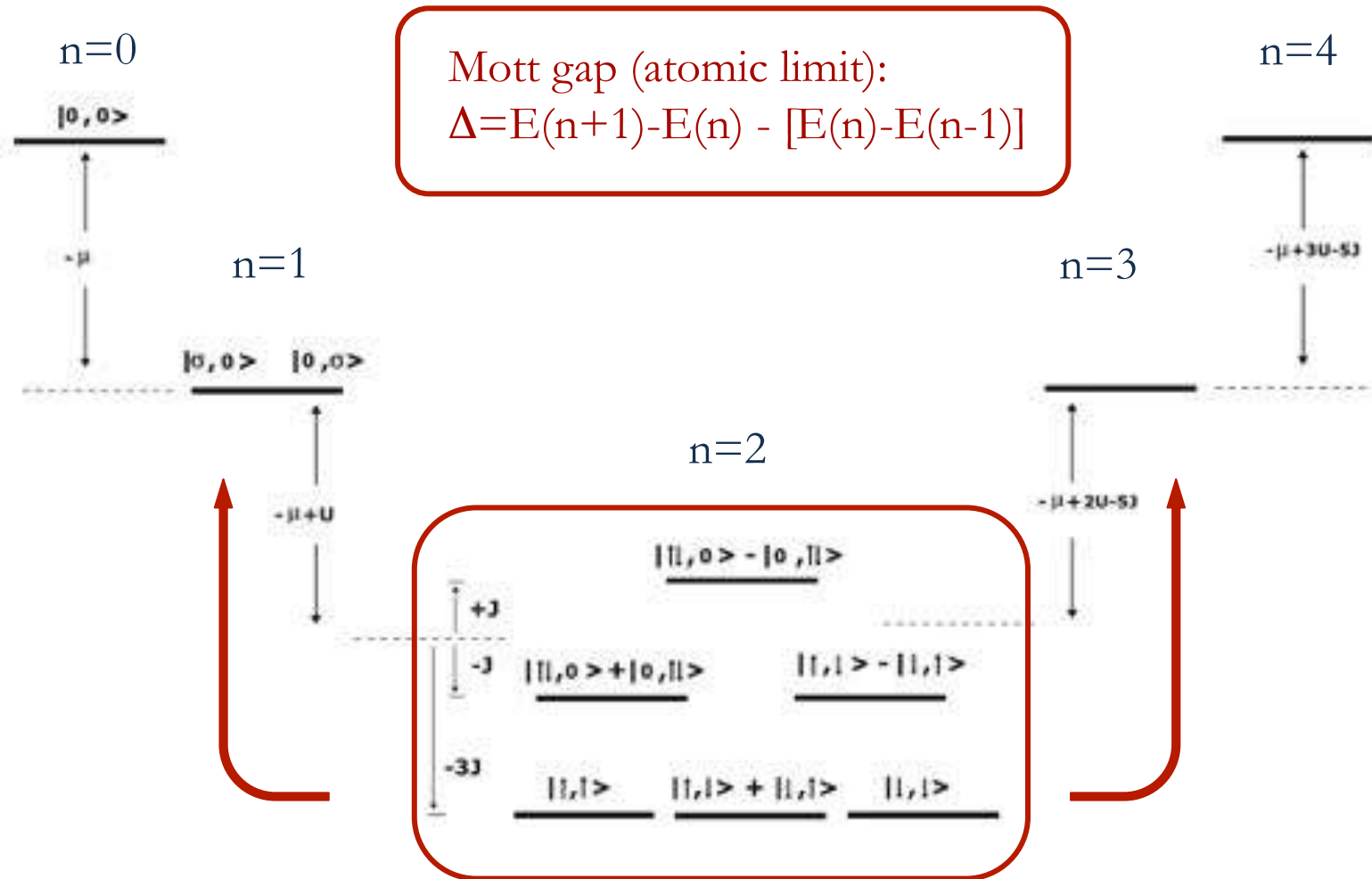


L. de' Medici, PRB 83, 205112 (2011)

see also

Werner, Gull and Millis PRB 79, 115119 (2009)

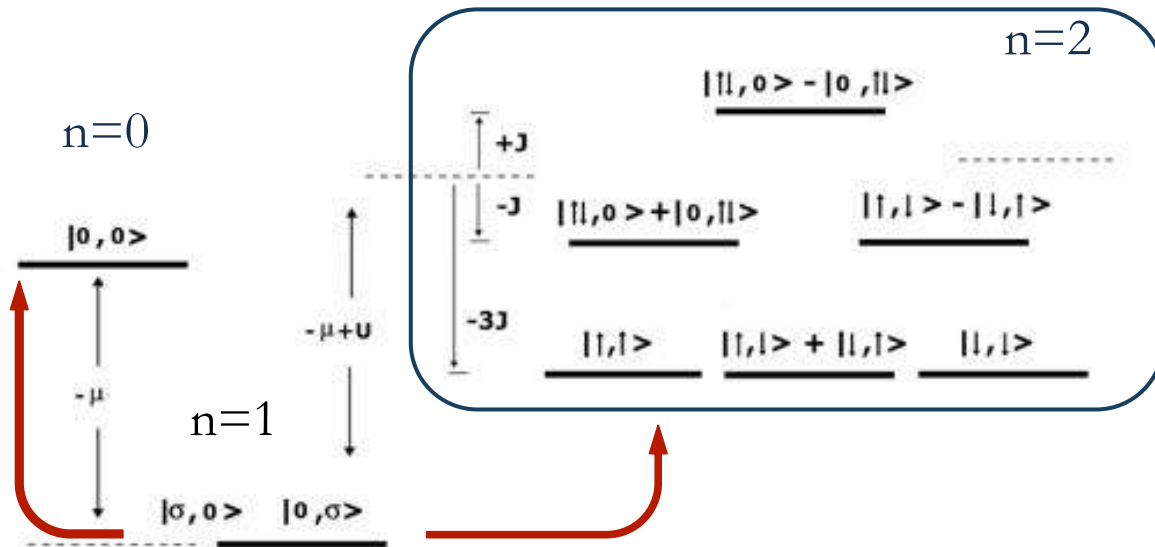
Hund's coupling changes the Mott gap: increased at $1/2$ filling



At half-filling $\Delta = U + J \rightarrow$ The gap increases with J
 Needs a smaller U for the Mott transition: U_c decreases

Hund's coupling changes the Mott gap: decreased for a generic filling

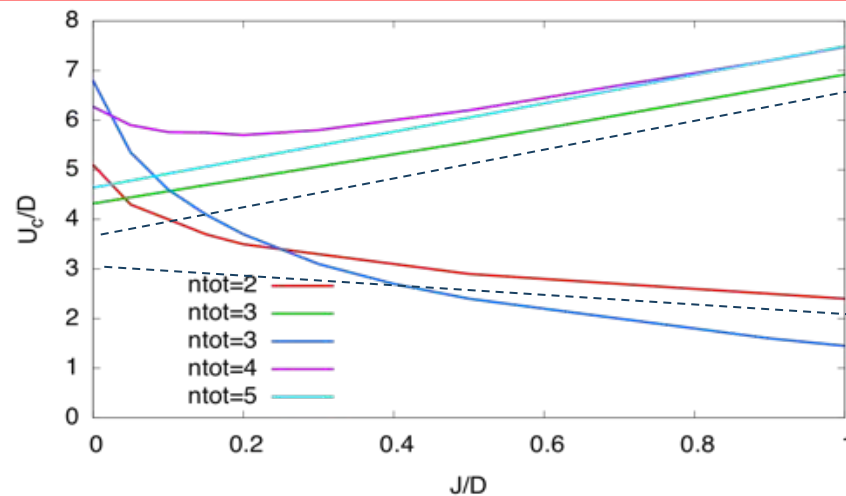
For $\langle n \rangle = 1$ the situation is inverted



$$\Delta = U - 3J$$

The gap is reduced by J

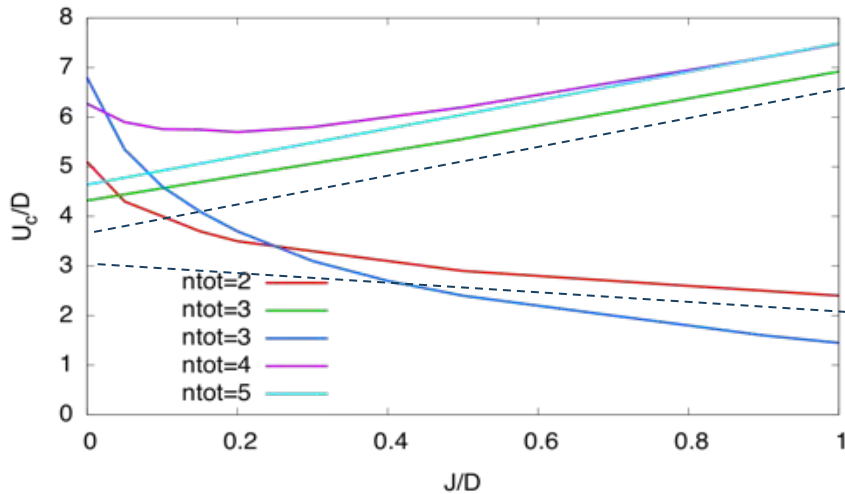
Needs a larger U for the Mott transition:
 Uc increases



$$\Delta = U - 3J$$

$$\Delta = U + J$$

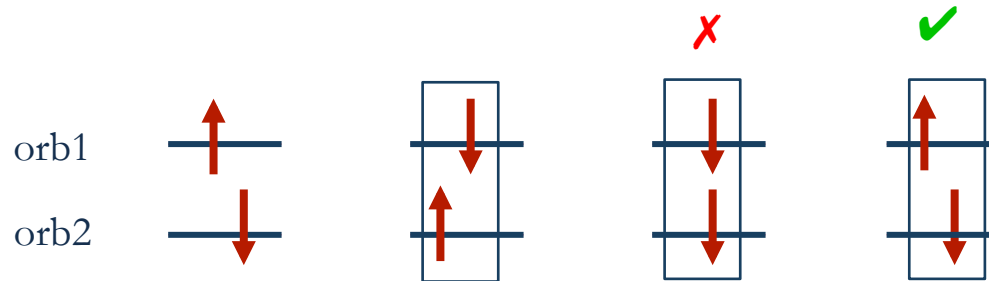
Suppression of orbital fluctuations by J



$$\Delta_{at} = U - 3J$$

$$\Delta_{at} = U + J$$

In all cases different from one electron ($n=1$) or one hole ($n=2M-1$) filling, there is a fast suppression of U_c at small J

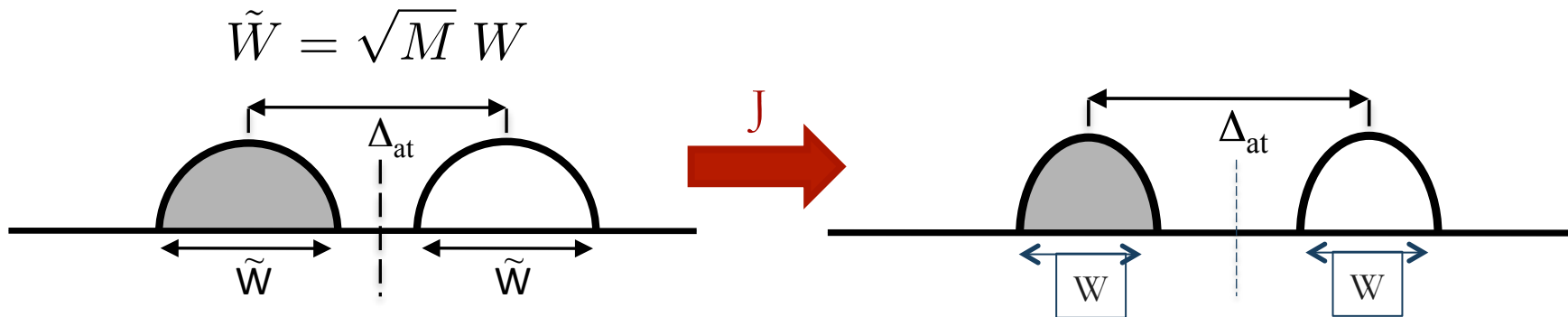


$$\Delta = U + J - W$$

$$\rightarrow U_c = W - J$$

$$= U_c(N = 1) - J$$

J limits again the hopping channels, smaller dispersion



Ground-state degeneracy and hopping processes

Both the Hubbard band widths and the quasiparticle mass are governed by the same hopping processes which are the less effective the lower the ground-state degeneracy

Hund's coupling lowers the ground-state degeneracy



- reduces the width Hubbard band
- reduces the quasiparticle weight (enhances the effective mass)

2 orbitals		
n	ground state degeneracy	
	J=0	finite J
0 (or 4)	1	1
1 (or 3)	4	4
2	6	3

3 orbitals		
n	ground state degeneracy	
	J=0	finite J
0 (or 6)	1	1
1 (or 5)	6	6
2 (or 4)	15	9
3	20	4

orbital decoupling mechanism

LdM and Capone in “The Iron-pnictide superconductors”, Springer book 2017
 see also Fanfarillo and Bascones, PRB 92 075136 (2015)

2 orbitals at half-filling – atomic limit

$J=0$

$J \neq 0$

ground state
6 x degenerate

$$\begin{array}{l}
 |\uparrow\downarrow, 0\rangle \quad |0, \uparrow\downarrow\rangle \\
 (|\uparrow, \downarrow\rangle - |\downarrow, \uparrow\rangle)/\sqrt{2} \\
 |\downarrow, \downarrow\rangle \quad (|\uparrow, \downarrow\rangle + |\downarrow, \uparrow\rangle)/\sqrt{2} \quad |\uparrow, \uparrow\rangle
 \end{array}$$



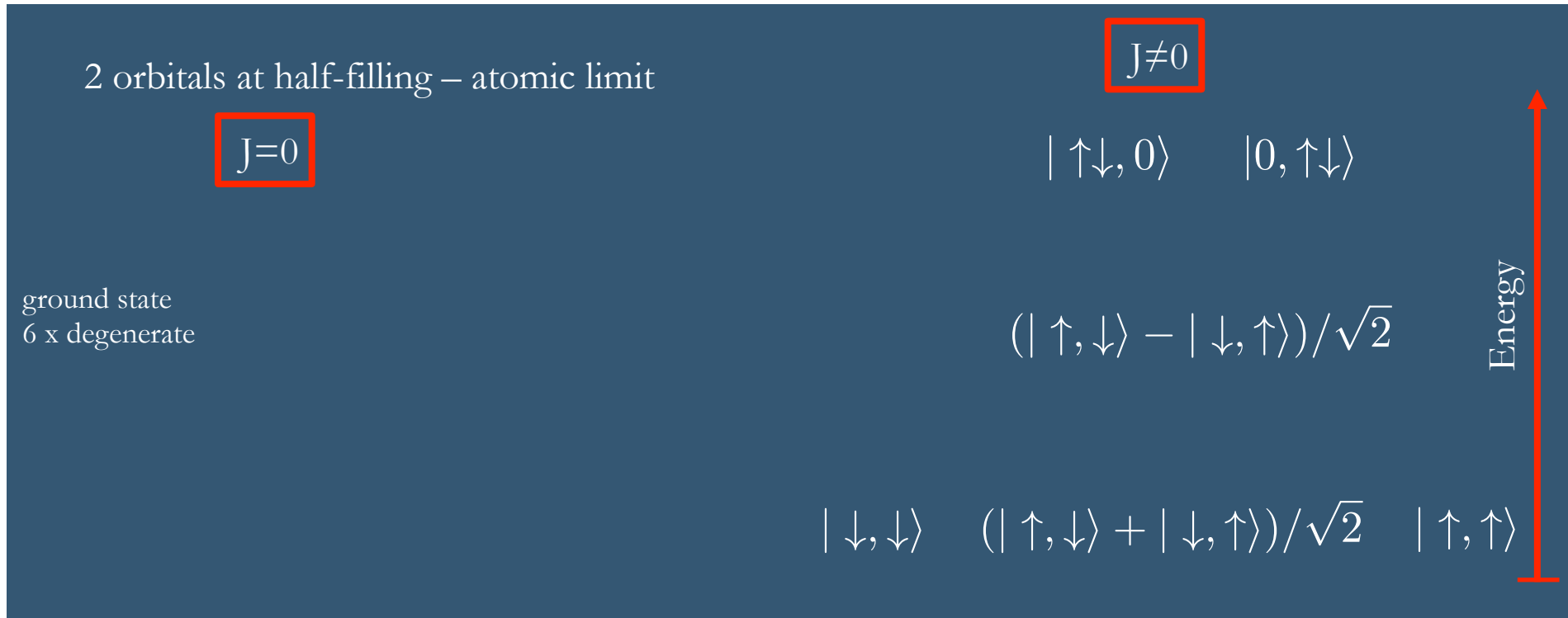
Fermi-liquid coherence (DMFT perspective): 2-orbital Anderson Impurity model
 Schrieffer –Wolff transformation -> Kondo model -> Kondo Temperature T_K

The low-energy, high-spin sector, allowed t^2 processes are only diagonal:
 T_K is diagonal in orbital space (i.e. it differs if $t_1 \neq t_2$)!

Schrieffer, J. Appl. Phys. 1967

orbital decoupling mechanism

LdM and Capone in “The Iron-pnictide superconductors”, Springer book 2017
 see also Fanfarillo and Bascones, PRB 92 075136 (2015)



Fermi-liquid coherence (DMFT perspective): 2-orbital Anderson Impurity model
 Schrieffer –Wolff transformation \rightarrow Kondo model \rightarrow Kondo Temperature T_K

The low-energy, high-spin sector, allowed t^2 processes are only diagonal:
 T_K is diagonal in orbital space (i.e. it differs if $t_1 \neq t_2$)!

Schrieffer, J. Appl. Phys. 1967

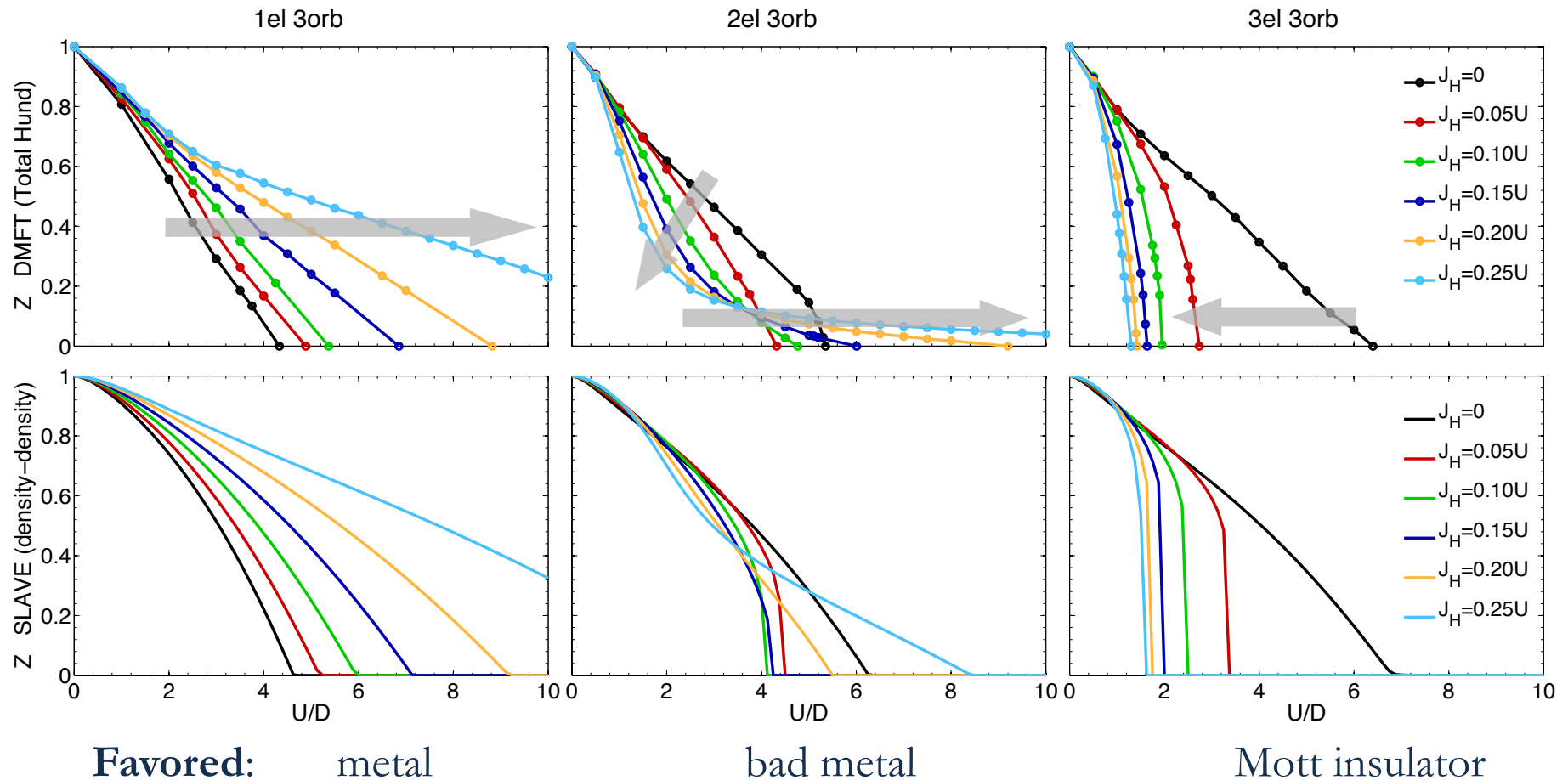
Analytical Slave-spin results

$$\bar{\epsilon}_0 \equiv \sum_{\mathbf{k}} \epsilon_{\mathbf{k}} \langle f_{\mathbf{k}\sigma}^\dagger f_{\mathbf{k}\sigma} \rangle_f \quad \text{bare kinetic energy}$$

- 1-band Hubbard $U_c = -16\bar{\epsilon}_0$ (=3.39 for Bethe W=2D)
- 2-band Hubbard (J=0) $U_c = -24\bar{\epsilon}_0$ (=5.09 for Bethe W=2D)
- N-band Hubbard (J=0) $U_c = -8(N + 1)\bar{\epsilon}_0$
- 2-band Hubbard (J≠0, large J):
 - Kanamori interaction (w/ spin-flip and pair-hopping terms)
$$U_c(N = 2) = -16\bar{\epsilon}_0 - J = U_c(N = 1) - J$$
 - density-density interaction
$$U_c(N = 2) = -8\bar{\epsilon}_0 - J = U_c(N = 1)/2 - J$$

3-band Hubbard model (semicircular DOS)

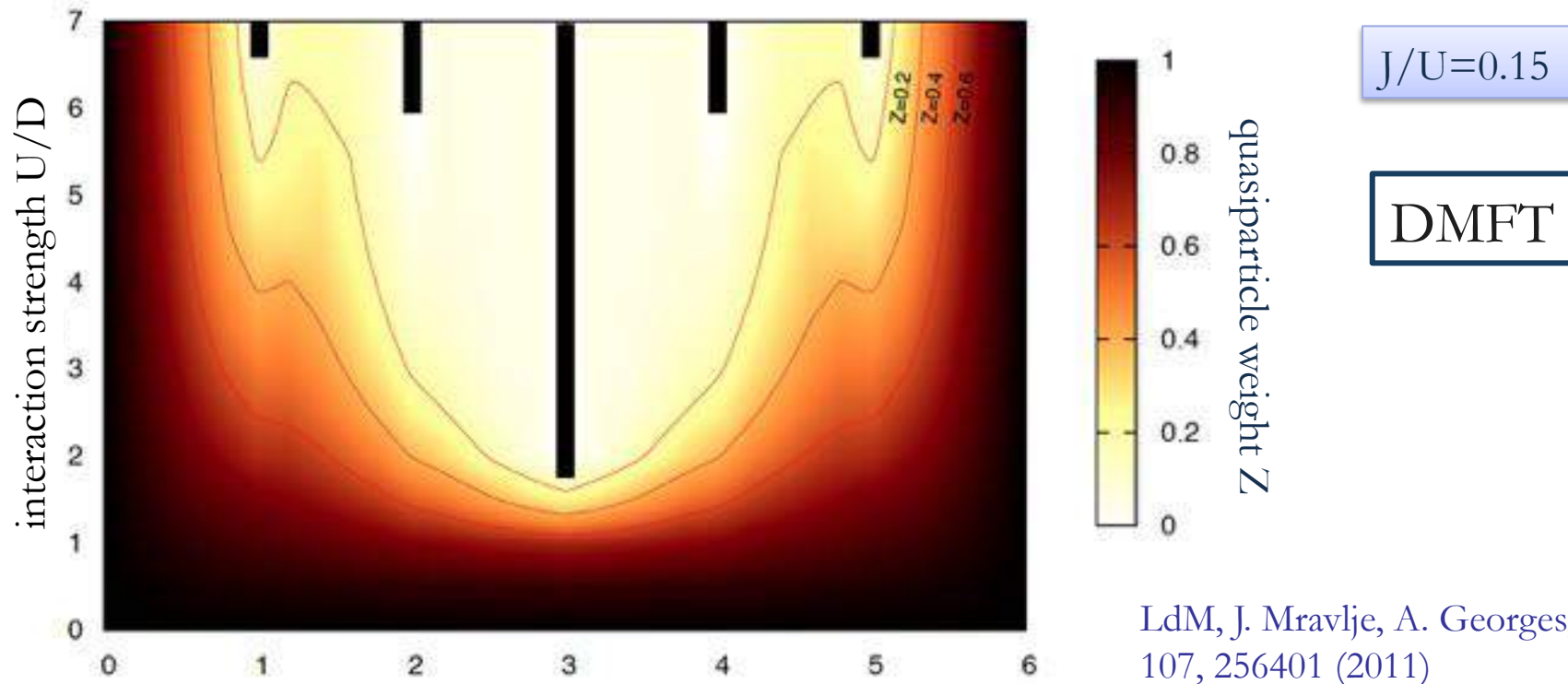
$M=3$ orbitals (relevant for t_{2g} materials)



LdM, J. Mravlje, A. Georges, PRL 107, 256401 (2011)

Fanfarillo and Bascones PRB 92, 075136 (2015)

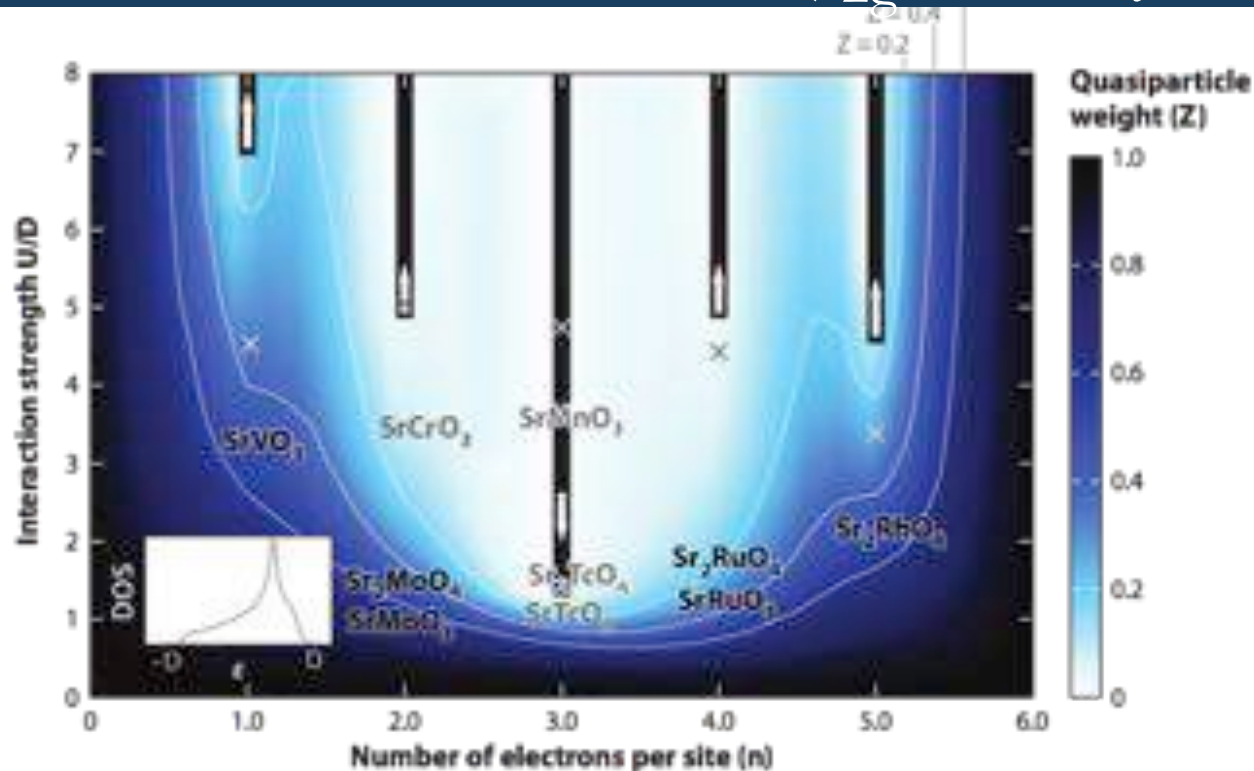
3-band Hubbard model (semicircular DOS)



Number N of electrons in M orbitals	Degeneracy of atomic ground-state	Mott gap	Correlations	Materials behaviour promoted by J
one electron or one hole ($N = 1, 2M - 1$)	unaffected	reduced	diminished	metallic
half-filled ($N = M$)	reduced	increased	increased	insulating
All other cases ($N \neq 1, M, 2M - 1$)	reduced	reduced	Conflicting effect (see text)	bad metallic

Table I: The effects of an increasing Hund's rule coupling on the degree of correlations.

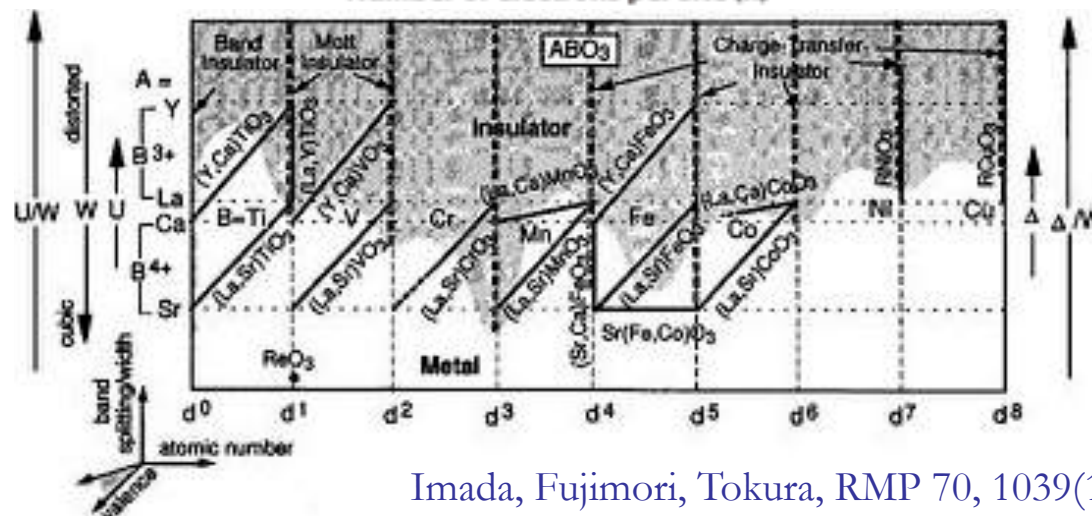
3-band Hubbard model (t_{2g} density of states)



$J/U=0.15$

DMFT

- 103 cubic
- 214 tetragonal (further splitting)



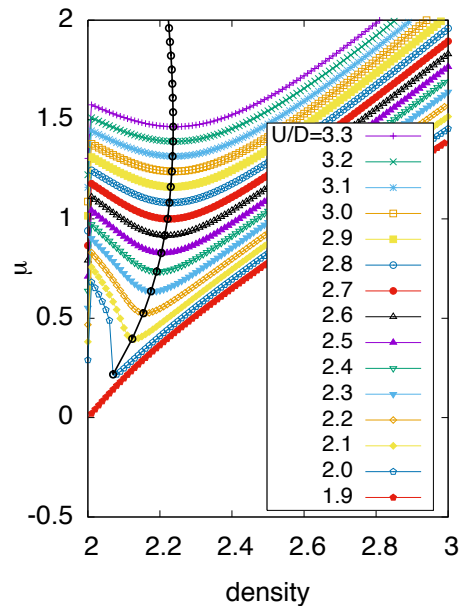
A. Georges, LdM, J. Mavrlje, Annual Reviews Cond. Mat. 4, 137 (2013)

Imada, Fujimori, Tokura, RMP 70, 1039(1998)

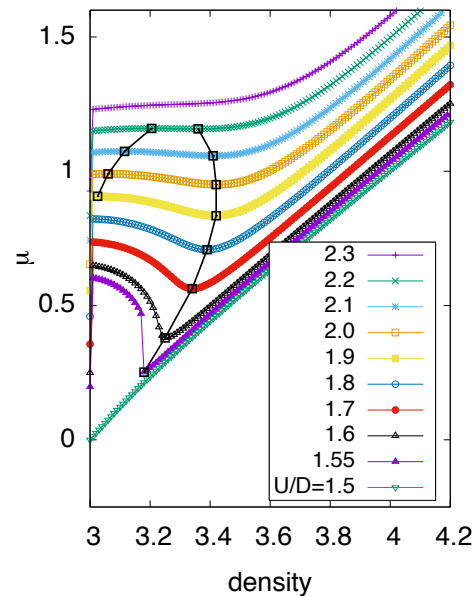
Compressibility in 2/3/5-orbital Hubbard model

$J/U=0.25$

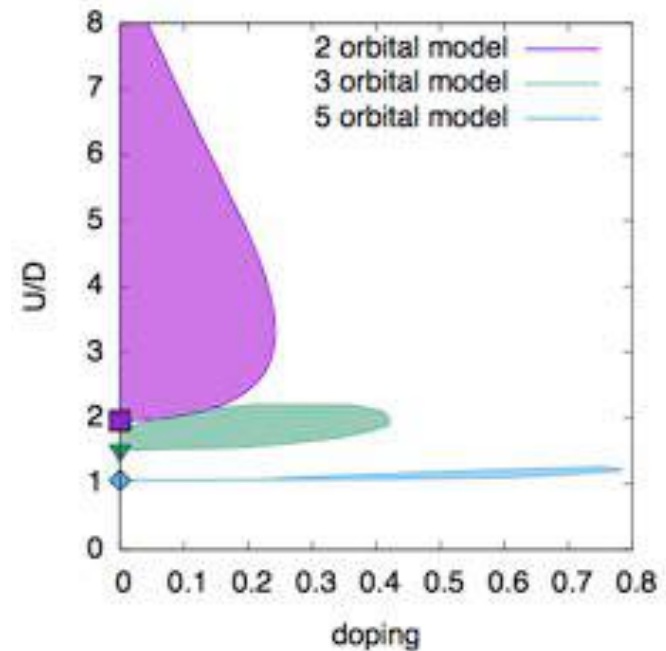
LdM, PRL 118 (2017)



2 orbitals



3 orbitals
(5 orb analogous)

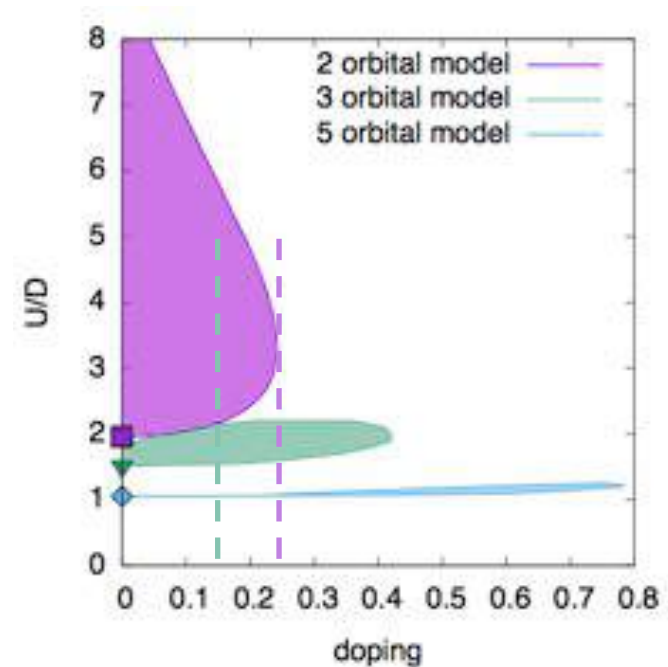
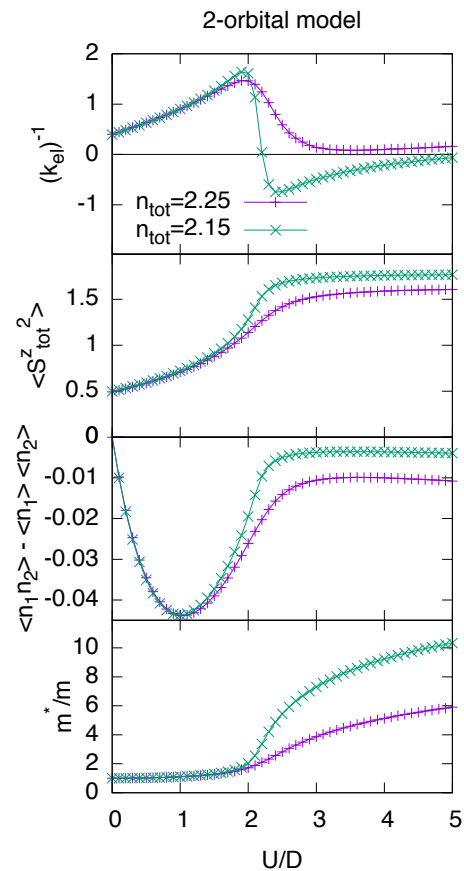


$$\chi = \frac{dn}{d\mu}$$

Divergence of the compressibility on a cross-over line departing from the Mott transition at half filling

Hund's metal frontier and enhanced compressibility

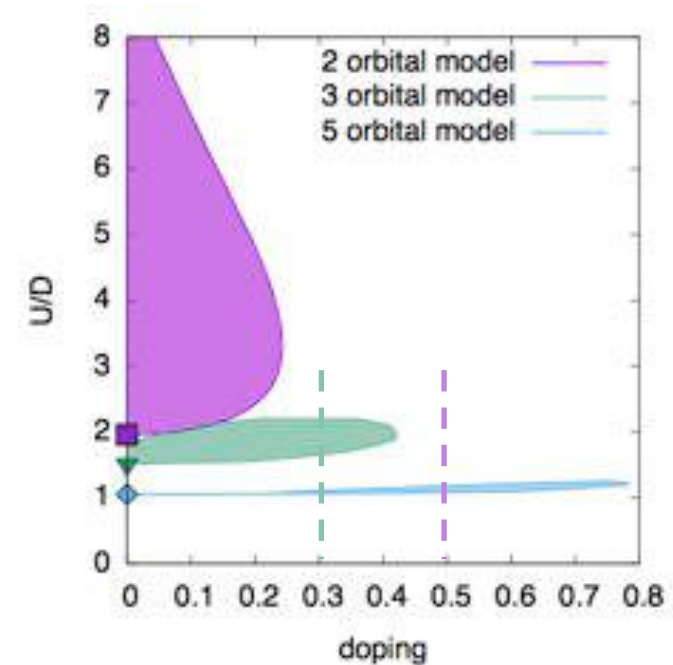
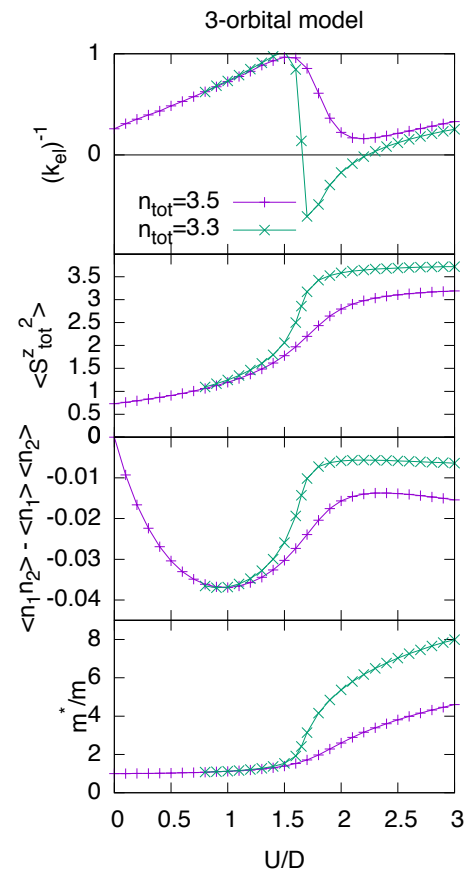
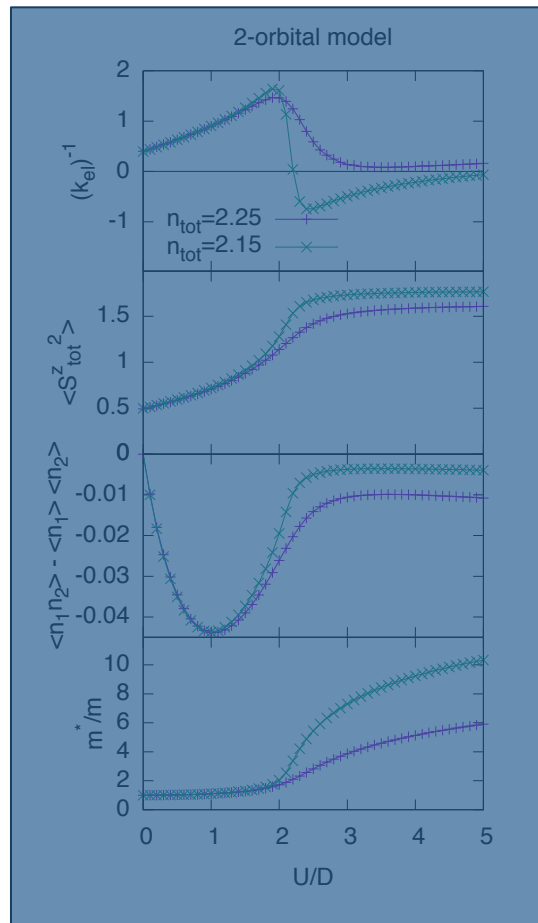
LdM, PRL 118 (2017)



The enhanced/divergent compressibility always occurs near
(just inside) the Hund's metal frontier

Hund's metal frontier and enhanced compressibility

LdM, PRL 118 (2017)



The enhanced/divergent compressibility always occurs near
(just inside) the Hund's metal frontier

Enhanced compressibility and superconductivity

In a Fermi liquid:

- $\chi = \frac{\chi_0/Z}{1 + F_0^s}$ If χ diverges for a finite $Z \rightarrow F_0^s < 0$
→ attraction ($q=0, \omega \rightarrow 0$) between quasiparticles

- in presence of some electron-boson coupling:
(Ward identity for the density vertex)

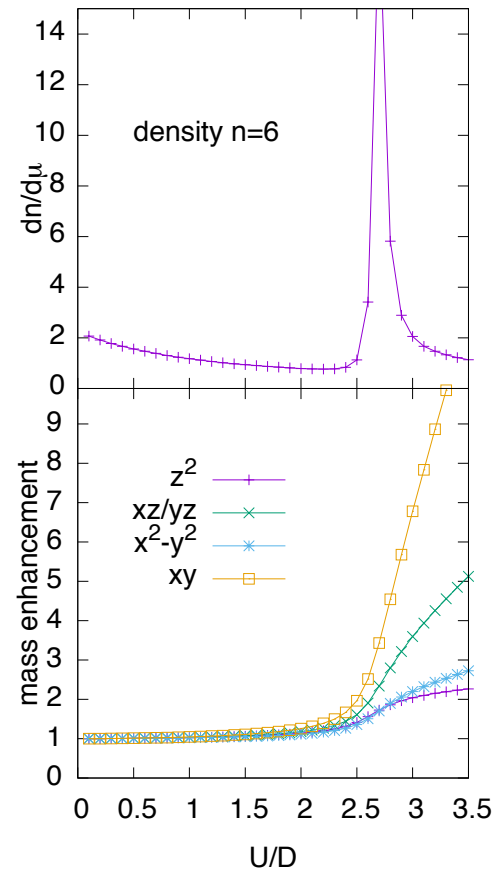
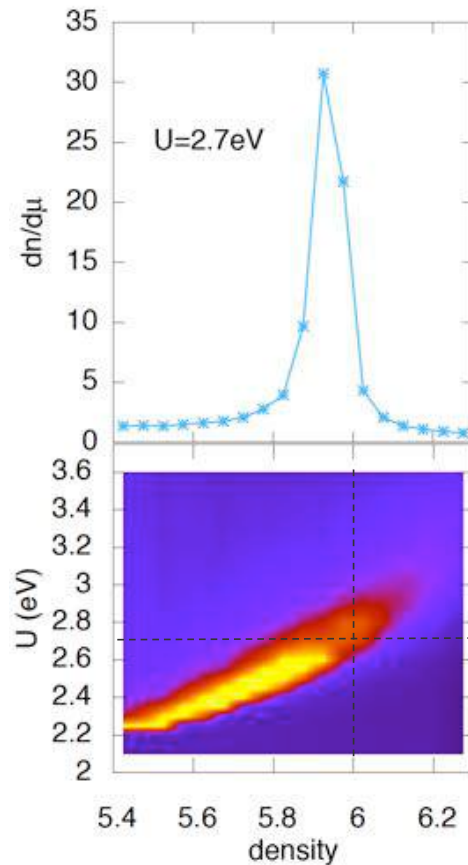
$$\Lambda(q \rightarrow 0, \omega = 0) = \frac{1}{Z(1 + F_0^s)} \rightarrow \text{enhanced} \sim \chi$$

- Phase separation → superconductivity scenario very much studied in the 90's for Cuprates
cfr: Emery, Kivelson and Lin, PRL 64, 475 (1990)
Grilli et al. PRL 67, 259 (1991)
Castellani, Di Castro and Grilli, PRL 75, 4650 (1995), ...

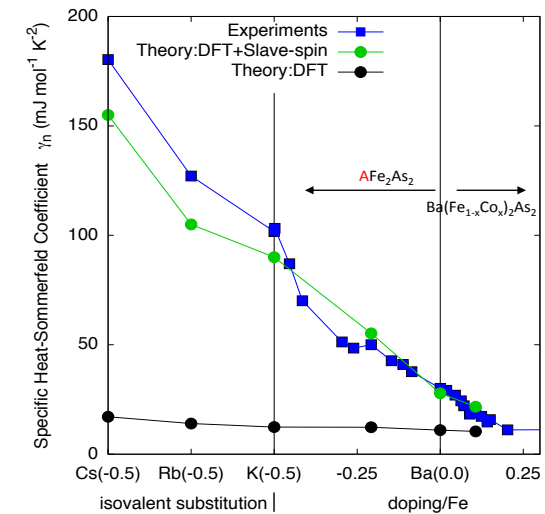
In this region not only the quasiparticle energies are renormalized non-trivially, but also their interactions (mutual and with low-energy bosons)!

Enhanced compressibility in BaFe_2As_2

LdM, PRL 118 (2017)



$U=2.7\text{eV}$, $J/U=0.25$
(interaction parameters that capture the Sommerfeld coefficient in the whole 122 family)

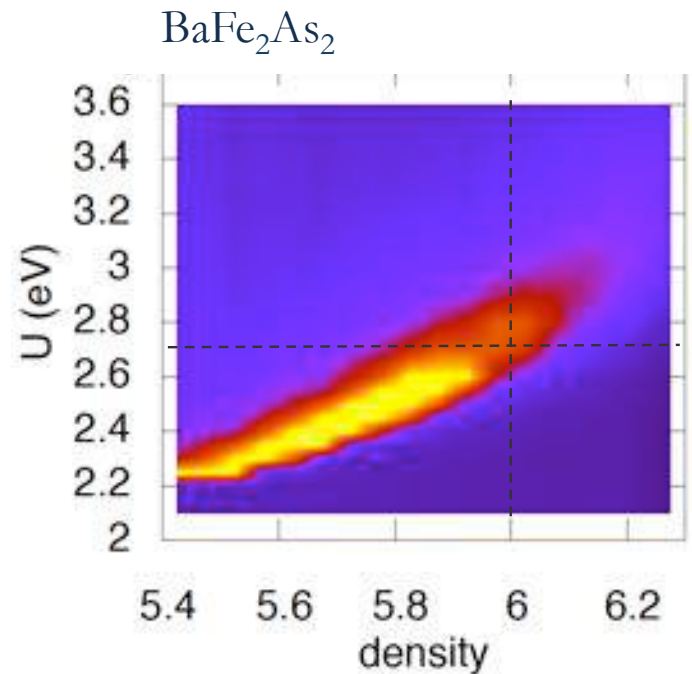


F. Hardy et al. PRB 94, 205113 (2017)

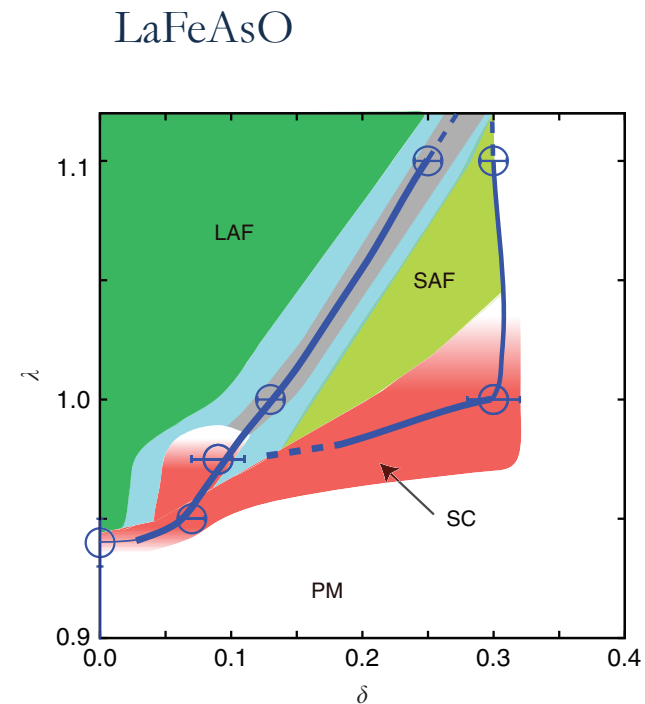
compressibility enhanced:

- in the doping zone where high- T_c happens
- at the entrance of the Hund's metal zone

Phase separation in VQMC



LdM, PRL 118, 167003 (2017)



Misawa and Imada, Nat. Comm 5, 5738 (2014)

In slave-spin mean-field it is simply a Fermi-liquid instability

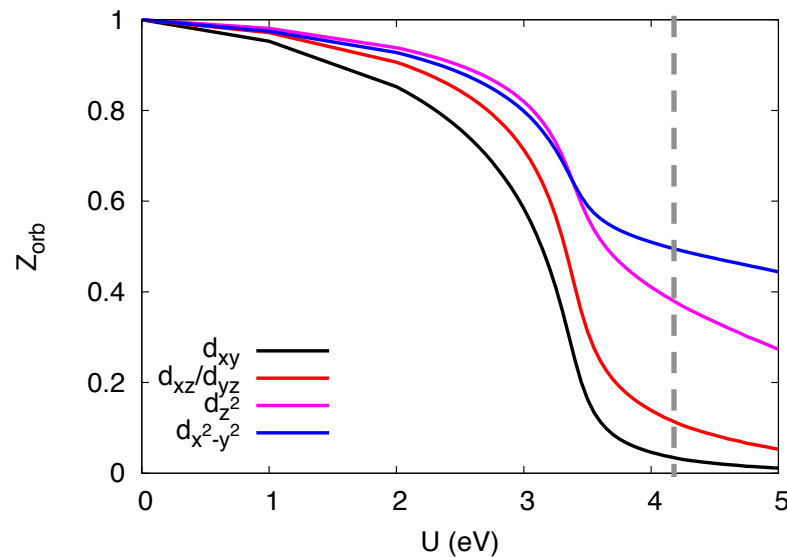
- independent of any symmetry breaking
- caused by Hund's coupling
- universal feature of Hund's metals

FeSe within DFT+Slave-Spin mean-field

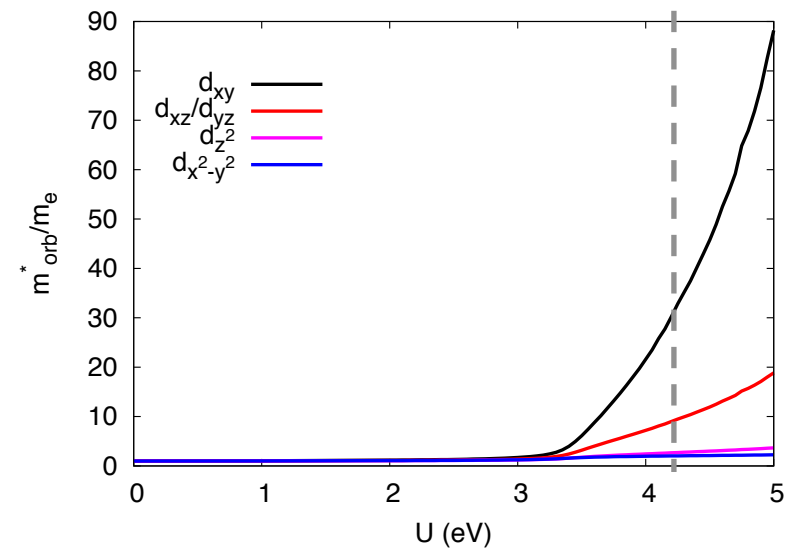
P. Villar Arribi
ESRF



quasiparticle weights



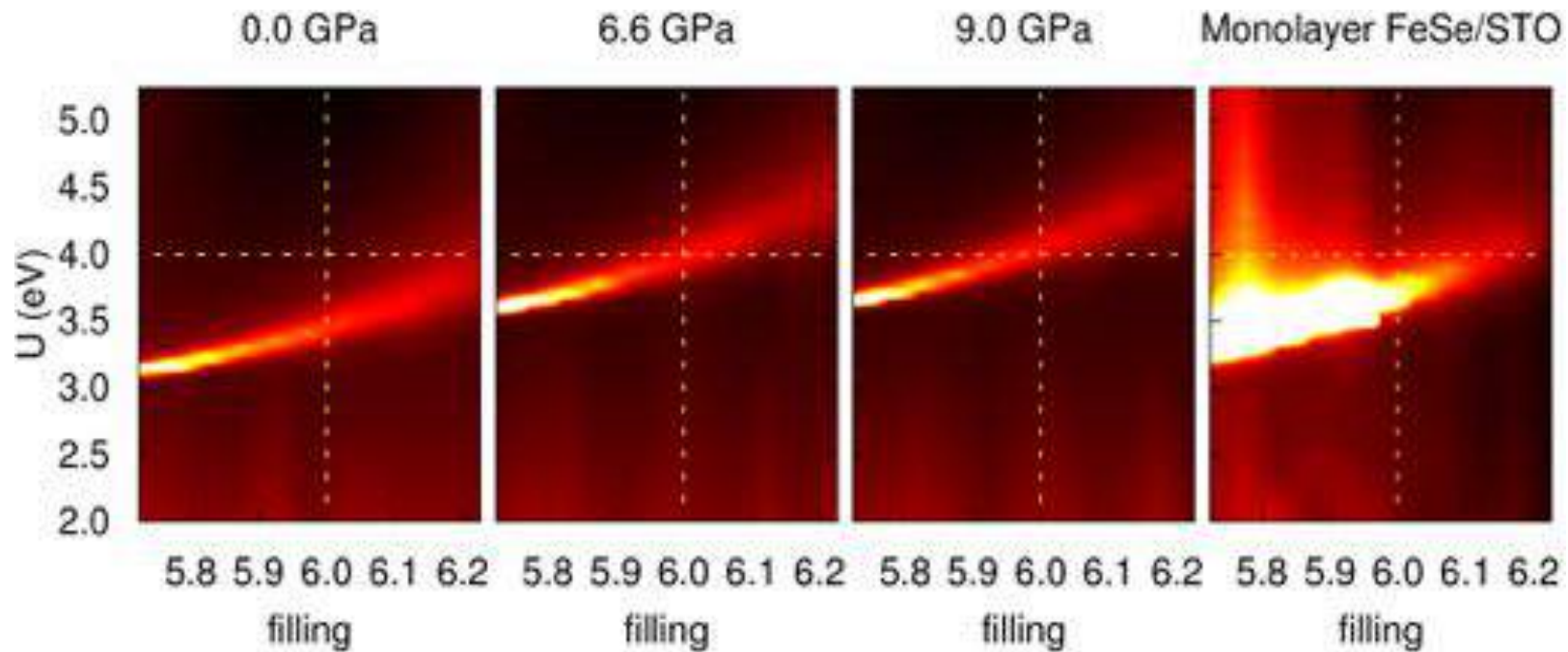
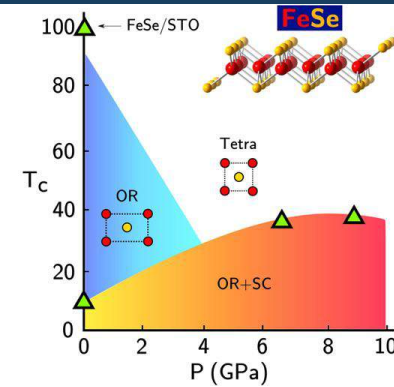
mass enhancements



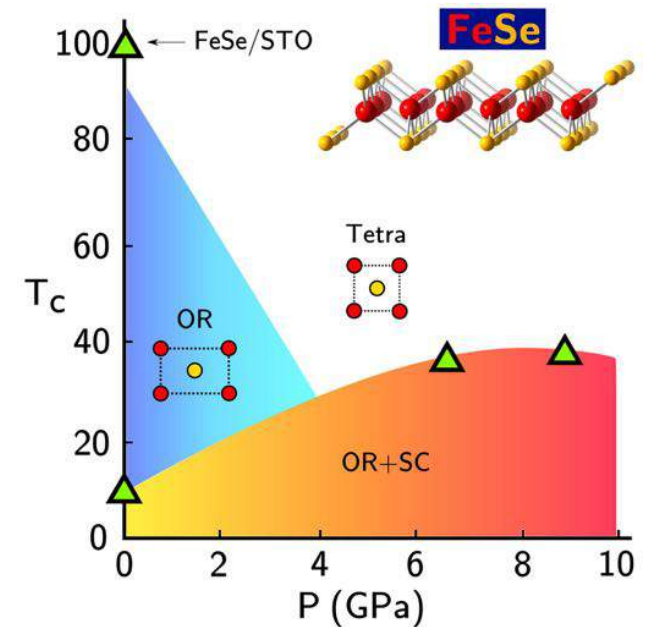
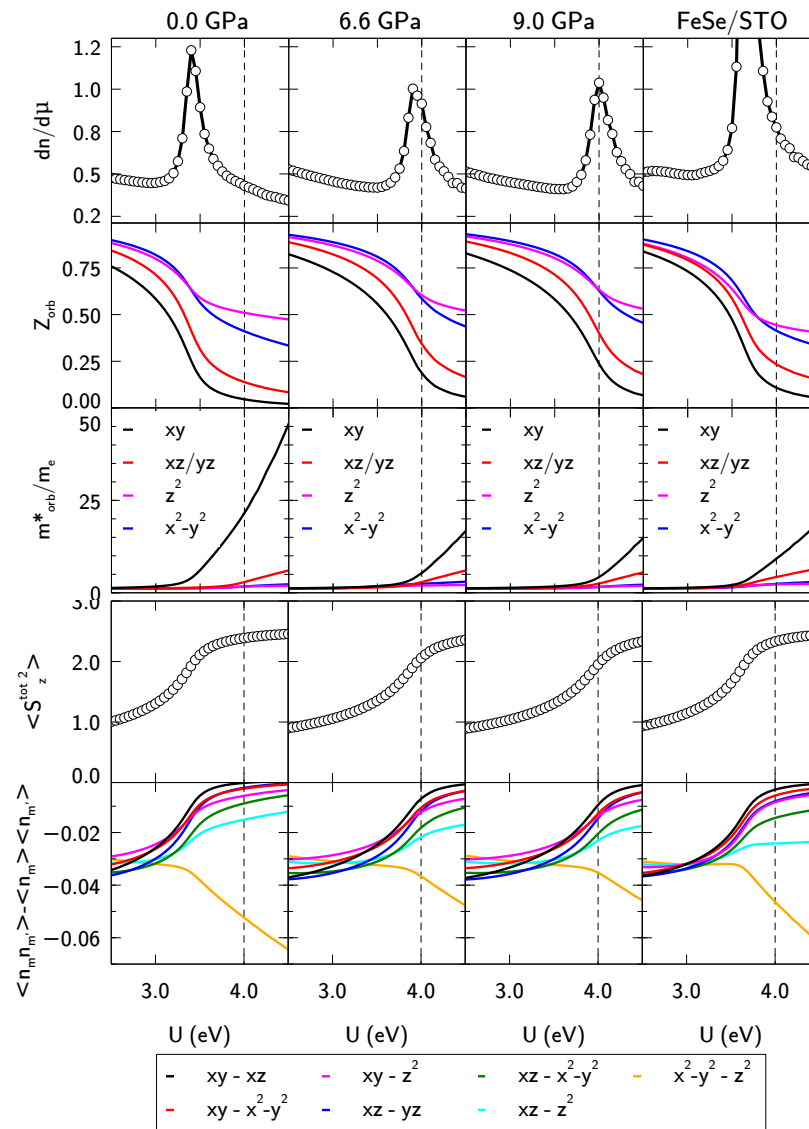
RPA-estimated U : bulk material deep within the “Hund’s metal” phase

FeSe/pressure & monolayer

FeSe: T_c grows under pressure
FeSe monolayer: highest claimed T_c



FeSe/pressure & monolayer



Conclusions and References

- **Hund's metals: high local moments, enhanced correlations, selective**
- **Onset of orbital selectivity easily highlights the Hund's metal frontier**

LdM, G. Giovannetti and M. Capone, PRL 112, 177001 (2014)

Selective Mott Physics as a key to Iron superconductors

LdM, *Weak AND strong correlations in Fe Superconductors*,

in "Iron-based Superconductivity", Springer Series in Material Sciences, Vol 211, pp 409-441 (2015)

- **Hund's induced phase-separation/enhanced qp interactions at Hund's metal frontier**
- **The mechanism can be associated to orbital decoupling**
- **This can favor superconductivity**

LdM, *Hund's induced Fermi-liquid instabilities and enhanced quasiparticle interactions*
PRL 118, 167003 (2017)

Pablo Villar-Arribi and LdM, *Enhanced compressibility in FeSe induced by Hund's coupling*, unpublished

- **Slave-spins:**

L. de' Medici and M. Capone in *The Iron Pnictide Superconductors*, Springer Series in Solid-State Sciences, Vol. 186, pp. 115-185, Mancini, F., Citro, R. (Eds) 2017.

